hypothesis because the proximal tubule marker-positive cell lies side by side with the distal tubule marker-positive cell in a single tubule (Figure 4g and h), and such chimeric tubule could not be made by the gradient of growth factors. From these findings, we postulate that each single cell possesses its cell fate to become proximal tubular cell or distal tubular cell. Further study is needed to clarify how these chimeric tubules differentiate to mature tubules (Figure 4h). Interestingly, all tubule epithelial cells positive for proximal tubule marker reside in the chimeric tubules in neonatal kidney, while some distal tubule marker-positive cells reside outside the area and are terminally differentiated (Figure 4a and c, arrowheads, H), indicating the possible sequence of differentiation.

USAG-1 expression decreases in tubular injury and increases in tubular regeneration

In the adult kidney, we demonstrated that the expression of USAG-1 colocalized with BMP-7 in DCTs (Figure 2a) and decreased in acute tubular injury (Figure 5). The reduction of USAG-1 expression in renal injury is not simply due to loss of tubular epithelial cells, because USAG-1 expression decreased rapidly in the very early stage of diseases, when morphological changes of tubular epithelial cells were not obvious (data not shown).

During the recovery from renal failure, regeneration of tubular epithelial cells occurs via proliferation and redifferentiation of surviving renal cells.[28] In the FA model, USAG-1 expression decreased during tubular injury, increased markedly during the regeneration of surviving cells, and returned to the basal level after redifferentiation was completed (Figure 6b). In contrast, the expression of BMP-7 increased gradually to the basal level after the initial dip during tubular injury (Figure 6b), resulting in a significant increase in the ratio between USAG-1 and BMP-7 during regeneration. Further examination with *USAG-1*-deficient mice is needed to clarify the role of USAG-1 in the regeneration of kidney injury.

USAG-1 could be a diagnostic marker for renal prognosis

In the clinical setting, prediction of renal prognosis is difficult even with histological examination, because damaged tubules and regenerating tubules are mixed in the single specimen, and are indistinguishable by morphology. Because USAG-1 is a negative regulator of the renoprotective action of BMP-7, we postulated that high expression of USAG-1 during kidney diseases might be a sign of poor renal prognosis. Because the coexistence of regenerating tubules and damaged tubules in FA nephrotoxicity model resembles the situation of renal biopsy in patients, we utilized the model and proved that high expression of USAG-1 in kidney biopsy in regenerating period correlated well with poor renal prognosis. Because the expression of USAG-1 is confined to the kidney, serum concentration of USAG-1 might reflect the renal expression level of USAG-1. In that case, blood test for USAG-1 concentration might be enough to predict renal prognosis and is suitable for health examination.

MATERIALS AND METHODS

Derivation of USAG-1/LacZ mice

To generate a null allele of *Sostdc1* (gene symbol for *USAG-1*), the coding sequence was replaced with the coding sequence of the marker gene LacZ, using Velocigene technology, essentially as described (Figure 1a).[29] PCR genotyping was performed in all subsequent studies to allow specific detection of the genotype (Figure 1b). The sequences of the primers used were as follows: primer A, CCTTCTCTGTGTTTTCACTCCG; primer B, TGATTCAGGGTGCTG TTGC; and lacZRev, CCGTAATGGGATAGGTCACG.

β-gal staining and *in situ* hybridization

β-gal staining and ISH were performed as described previously.[17,29] Probe for ISH was designed to contain the open reading frame with the following length and GC content: USAG-1, 1.0 kbp (GC 52.6%). Hybridization was detected using an anti-DIG AP conjugate (Roche, Basel, Switzerland) and NBT/BCIP solution (Roche).

Histological studies and immunostaining

The kidneys were fixed in Carnoy's solution, embedded in paraffin, and sections (4 μm thick) were stained with periodic acid-Schiff for routine histological examination. Frozen sections of the kidneys and primary kidney tubular cells were immunostained as previously described.[30] Reagents utilized were anti-NaKATPase α-1 antibody (Ab) (Upstate, Billerica, MA, USA), anti-calbindin D28K (Sigma, St Louis, MO, USA), anti-Tamm Horsfall Protein Ab (Biomedical Technologies Inc.), anti-aquaporin 1 Ab (Chemicon, Temecula, CA, USA), anti-aquaporin 2 Ab (Calbiochem, Darmstadt, Germany), FITC-conjugated lotus tetragonolobus agglutinin (LTA) (Sigma), anti-LacZ Ab (Cappel, Solon, OH, USA), and anti-NDRG1 Ab.[20] For double staining, immunostaining was performed before β-gal staining, to avoid the possibility that the deposition of X-gal interferes with antibody binding to the antigen.

Quantification of mRNA by real-time RT-PCR

Real-time reverse transcription (RT)-PCR was performed as described previously.[17] Specific primers were designed using Primer Express software (Applied Biosystems, Foster City, CA, USA). To compare the expression levels of different genes, we used modified real-time PCR by setting the standard curves with plasmids encoding each gene at various concentrations, and analyzed the copy number of each gene contained in kidney cDNA as previously described.[17] Serially diluted cDNA or plasmids were used to generate the standard curve for each primer, and the PCR conditions were as follows: 50 °C for 2 min, 95 °C for 10 min, then 95 °C for 15 s, and 60 °C for 1 min for 40 cycles.

Kidney disease models

Cisplatin nephrotoxicity was caused as described previously.[17] Briefly, cisplatin (20 mg kg^{-1}, Sigma-Aldrich) was administered by a single intraperitoneal injection to 8-week-old female C57BL/6J mice (SLC Japan, Shizuoka, Japan). FA nephrotoxicity was caused by a single intraperitoneal injection of FA (250 mg kg^{-1}, Sigma-Aldrich) in 0.15 M $NaHCO_3$ to 11-week-old male C57BL/6J mice. The kidneys were collected at days 0, 1, 4, 10, and 14, with at least three animals at each time point.

Animal use

All mice were housed in specific pathogen-free conditions. All animal experiments were performed in accordance with the institutional guidelines as well as the National Institutes of Health (NIH) guidelines.

Statistical analysis

All assays were performed in triplicate. Data were presented as mean ± s.d. Statistical significance was assessed by analysis of variance, followed by Fisher's protected LSD *post hoc* test. Correlation was determined by Spearman's correlation analysis.

ACKNOWLEDGMENTS

We thank Drs Y Nabeshima, E Nishi, and T Nakamura for valuable comments and discussion; S Tahara and A Yoshioka for experiments not included in the manuscript; and A Hosotani for technical assistance. This study was supported by grants-in-aid from the Ministry of Education, Culture, Science, Sports, and Technology of Japan (177090551); a Center of Excellence grant from the Ministry of Education, Culture, Science, Sports, and Technology of Japan; a research grant for health sciences from the Japanese Ministry of Health, Labor and Welfare; a grant from the Astellas Foundation for Research on Metabolic Disorders; a grant from the Novartis Foundation for the promotion of science; a grant from Kato Memorial Trust for Nambyo Research; a grant from Hayashi Memorial Foundation for Female Natural Scientists; and a grant from Japan Foundation for Applied Enzymology.

SUPPLEMENTARY MATERIAL

Figure S1. Relative expression of USAG-1 and other BMP antagonists to BMP-7 in kidney disease models.

Figure S2. Significant correlation was observed between *USAG-1* expression and future serum creatinine (day 14) in case that kidney biopsy was performed at day 10 but not at day 1 in folic acid nephrotoxicity (closed circles).

REFERENCES

1. Reddi AH. Bone morphogenetic proteins and skeletal development: the kidney-bone connection. *Pediatr Nephrol* 2000; **14**: 598–601.
2. Massague J, Chen YG. Controlling TGF-beta signaling. *Genes Dev* 2000; **14**: 627–644.
3. Dudley AT, Lyons KM, Robertson EJ. A requirement for bone morphogenetic protein-7 during development of the mammalian kidney and eye. *Genes Dev* 1995; **9**: 2795–2807.
4. Luo G, Hofmann C, Bronckers AL *et al.* BMP-7 is an inducer of nephrogenesis, and is also required for eye development and skeletal patterning. *Genes Dev* 1995; **9**: 2808–2820.
5. Dudley AT, Robertson EJ. Overlapping expression domains of bone morphogenetic protein family members potentially account for limited tissue defects in BMP7 deficient embryos. *Dev Dyn* 1997; **208**: 349–362.
6. Kalluri R, Neilson EG. Epithelial-mesenchymal transition and its implications for fibrosis. *J Clin Invest* 2003; **112**: 1776–1784.
7. Zeisberg M, Hanai J, Sugimoto H *et al.* BMP-7 counteracts TGF-beta1-induced epithelial-to-mesenchymal transition and reverses chronic renal injury. *Nat Med* 2003; **9**: 964–968.
8. Zeisberg M, Shah AA, Kalluri R. Bone morphogenic protein-7 induces mesenchymal to epithelial transition in adult renal fibroblasts and facilitates regeneration of injured kidney. *J Biol Chem* 2005; **280**: 8094–8100.
9. Wang S, Chen Q, Simon TC *et al.* Bone morphogenic protein-7 (BMP-7), a novel therapy for diabetic nephropathy. *Kidney Int* 2003; **63**: 2037–2049.
10. Wang S, de Caestecker M, Kopp J *et al.* Renal bone morphogenetic protein-7 protects against diabetic nephropathy. *J Am Soc Nephrol* 2006; **17**: 2504–2512.
11. Gould SE, Day M, Jones SS *et al.* BMP-7 regulates chemokine, cytokine, and hemodynamic gene expression in proximal tubule cells. *Kidney Int* 2002; **61**: 51–60.
12. Lin J, Patel SR, Cheng X *et al.* Kielin/chordin-like protein, a novel enhancer of BMP signaling, attenuates renal fibrotic disease. *Nat Med* 2005; **11**: 387–393.
13. Reddi AH. Interplay between bone morphogenetic proteins and cognate binding proteins in bone and cartilage development: noggin, chordin and DAN. *Arthritis Res* 2001; **3**: 1–5.
14. Yanagita M. BMP antagonists: their roles in development and involvement in pathophysiology. *Cytokine Growth Factor Rev* 2005; **16**: 309–317.
15. Yanagita M. Modulator of bone morphogenetic protein activity in the progression of kidney diseases. *Kidney Int* 2006; **70**: 989–993.
16. Yanagita M, Oka M, Watabe T *et al.* USAG-1: a bone morphogenetic protein antagonist abundantly expressed in the kidney. *Biochem Biophys Res Commun* 2004; **316**: 490–500.
17. Yanagita M, Okuda T, Endo S *et al.* Uterine sensitization-associated gene-1 (USAG-1), a novel BMP antagonist expressed in the kidney, accelerates tubular injury. *J Clin Invest* 2006; **116**: 70–79.
18. Sasaki S, Fushimi K, Saito H *et al.* Cloning, characterization, and chromosomal mapping of human aquaporin of collecting duct. *J Clin Invest* 1994; **93**: 1250–1256.
19. Cho EA, Patterson LT, Brookhiser WT *et al.* Differential expression and function of cadherin-6 during renal epithelium development. *Development* 1998; **125**: 803–812.
20. Okuda T, Higashi Y, Kokame K *et al.* Ndrg1-deficient mice exhibit a progressive demyelinating disorder of peripheral nerves. *Mol Cell Biol* 2004; **24**: 3949–3956.
21. Wakisaka Y, Furuta A, Masuda K *et al.* Cellular distribution of NDRG1 protein in the rat kidney and brain during normal postnatal development. *J Histochem Cytochem* 2003; **51**: 1515–1525.
22. Long DA, Woolf AS, Suda T *et al.* Increased renal angiopoietin-1 expression in folic acid-induced nephrotoxicity in mice. *J Am Soc Nephrol* 2001; **12**: 2721–2731.
23. Gupta IR, Piscione TD, Grisaru S *et al.* Protein kinase A is a negative regulator of renal branching morphogenesis and modulates inhibitory and stimulatory bone morphogenetic proteins. *J Biol Chem* 1999; **274**: 26305–26314.
24. Dressler GR. The cellular basis of kidney development. *Annu Rev Cell Dev Biol* 2006; **22**: 509–529.
25. Cheng HT, Kopan R. The role of Notch signaling in specification of podocyte and proximal tubules within the developing mouse kidney. *Kidney Int* 2005; **68**: 1951–1952.
26. Chen L, Al-Awqati Q. Segmental expression of Notch and Hairy genes in nephrogenesis. *Am J Physiol Renal Physiol* 2005; **288**: F939–F952.
27. McLaughlin KA, Rones MS, Mercola M. Notch regulates cell fate in the developing pronephros. *Dev Biol* 2000; **227**: 567–580.
28. Thadhani R, Pascual M, Bonventre JV. Acute renal failure. *N Engl J Med* 1996; **334**: 1448–1460.
29. Valenzuela DM, Murphy AJ, Frendewey D *et al.* High-throughput engineering of the mouse genome coupled with high-resolution expression analysis. *Nat Biotechnol* 2003; **21**: 652–659.
30. Yanagita M, Arai H, Ishii K *et al.* Gas6 regulates mesangial cell proliferation through Axl in experimental glomerulonephritis. *Am J Pathol* 2001; **158**: 1423–1432.
31. Thimmappaya B, Zain BS, Dhar R *et al.* Nucleotide sequence of DNA template for the 3′ ends of SV40 mRNA. II. The sequence of the DNA fragment *Eco*RII-F and a part of *Eco*RII-H. *J Biol Chem* 1978; **253**: 1613–1618.
32. Adra CN, Boer PH, McBurney MW. Cloning and expression of the mouse pgk-1 gene and the nucleotide sequence of its promoter. *Gene* 1987; **60**: 65–74.

特集：腎における細胞内シグナル伝達と病態生理

【腎障害・壊死におけるシグナル伝達】

抗生物質と細胞毒*

市村隆治**　増田智先***

はじめに：細胞毒による尿細管上皮細胞の損傷と細胞死

急性腎障害において，虚血と細胞毒は重要な尿細管上皮細胞の損傷，細胞死の原因であり，その発症メカニズムにおける細胞内シグナリングの役割を理解することはきわめて重要と考えられる。同時に，尿細管上皮細胞の損傷や細胞死に対する防御方法をさぐることもできる。

抗生物質や細胞毒，さらには虚血による腎障害では，それらの刺激に特に感受性の強い近位尿細管上皮細胞が標的となる。そこで，抗生物質とそのほかの腎特異的な細胞毒による近位尿細管上皮細胞の損傷メカニズムを理解するためには，細胞の普遍的な損傷のメカニズムと近位尿細管上皮細胞の分化機能（特に毒物の分布，濃縮）に関係した損傷メカニズムの両方を考慮しなければならない。本稿でとりあげる抗生物質と細胞毒による毒性は近位尿細管上皮細胞内に濃縮されることによって発現するということからも明らかであろう。

腎毒性の重要な原因となる，抗生物質とそのほかの細胞毒として抗癌薬であるシスプラチンをとりあげて，これらの物質の腎毒性発現における細胞内シグナリングの役割を検討したい。

また，われわれの研究成果を例としてシグナリングを利用した細胞毒性への防御のメカニズムについて述べる。

Ⅰ．毒物と細胞死―細胞死には細胞内シグナリングの役割をもつ

細胞の生存，恒常性（ホメオスタシス）の維持，そして細胞死において，細胞内シグナリングはきわめて重要な役割を果たしている。細胞の生死は，生命維持と細胞死という側面の細胞内シグナリングのバランスによって成り立っている[1]。近位尿細管上皮細胞のように分化して特異的な働きをしている細胞であれば，その分化と機能の恒常性の維持もまた細胞内シグナリングによって調節されている。一般に理解されている細胞毒性のメカニズムは，この細胞内オルガネラの破壊（DNA やミトコンドリアの損傷など）によってもたらされる細胞のバランス機能の攪乱によるものである。この毒性メカニズムを理解するうえで大切なことは，毒物によってどの細胞内シグナリング，パスウェイが標的となって，またどのような形で攪乱されているのかということである。このように「恒常性」は，以下に述べるように細胞死シグナリングの抑制，または促進などといった細胞の生死を支

* Antibiotics and nephrotoxicants
key words：アポトーシス，ネクローシス，オートファジー，小胞体ストレス，ゲンタマイシン，シスプラチン
** Renal Division, Department of Medicine, Brigham and Women's Hospital, Harvard Medical School
ICHIMURA Takaharu
〔4 Blackfan Circle, Boston, MA 02115, USA〕
*** 京都大学医学部附属病院薬剤部　MASUDA Satohiro

配する重要な機能を含んでいる。したがって，細胞毒性の発現という細胞の損傷と死を招く深刻な刺激下において，生存シグナリングによる調節メカニズムは細胞毒に対する主要な応答機能と考えられる[2]。すなわち，細胞毒性発現の分子メカニズムや，それを阻止するための方法論を見出すには，細胞内で営まれるシグナリングの理解が大切である。

近年のトキシコゲノミクスやプロテオミクスといった研究も，未知の毒性の標的や毒性への応答を見出すための網羅的探索法として行われている。

II．細胞死のタイプ，メカニズムと細胞内シグナリング

最近の研究によって[3]，いずれのタイプの細胞死もプログラム細胞死であることがわかってきている。プログラム細胞死とは死のプロセスが細胞内のメカニズムによって制御されていて，単純なシステムの破綻ではないことをいう。ここで細胞死のタイプとその細胞内シグナリング，毒性の標的や毒性への応答に重要ないくつかの細胞内シグナリングメカニズムを簡単に紹介する。

1．アポトーシス（図1）

最も代表的なプログラム細胞死であり，染色体DNAの断片化によって特徴づけられる。アポトーシスはホメオスタシスの一部であり正常な組織や発生の途上で常に起こっているが，毒性作用によっても誘導される[1,3]。デスリガンドとデスリセプター（受容体）を介した外因性のアポトーシスと内因性のシグナルによるアポトーシスの2つのタイプがある。

主に内因性のアポトーシスによる細胞内シグナリングメカニズムを簡単に説明する。さまざまな細胞ストレスが原因となってアポトーシスの引き金（トリガー）となる因子の活性化が起こる。

p53はアポトーシスのトリガー因子の代表とされており，活性化されたこれらの刺激がBcl2ファミリーの蛋白質を活性化する。特にBax，Bad，Bakなどのアポトーシスを促進させる蛋白質が，このシグナリング経路で重要な役割を担うミトコンドリアを刺激する。Bcl2や$BcLX_L$はこれを阻害する作用をもつ。ミトコンドリアの刺激によって，チトクロムCやOmi，Smacなどアポトーシスシグナルを促す重要な蛋白質の漏出が誘導される。漏出されたチトクロムCはカスパーゼ9，そして染色体DNAや細胞内蛋白質の断片化を媒介するカスパーゼ3と7の活性化によるアポトーシスを引き起こす。OmiやSmacはカスパーゼ活性化の促進という役割を担う。細胞の生命維持にとって，このアポトーシスシグナルの抑制が重要であり，いくつかの抑制機構が知られている。Bcl2などの阻害因子は最もよく知られているが，そのほか蛋白質リン酸化酵素でありMAPキナーゼファミリーに属するERKはアポトーシスを抑制する機能を有する[4]。一方，同じMAPキナーゼでも，JNKやp38はアポトーシスを促進する作用がある。また，PI3KやAKTもアポトーシスを抑制する。

2．ネクローシス

細胞内小器官の膨化によって特徴づけられる。従来，制御不能な細胞死と理解されてきたが，ネクローシスもまたプログラム細胞死の1つとして最近理解されつつある[3,5]。病理学的には，ヒトや実験動物の虚血または腎毒性による急性腎障害（AKI）において，このタイプの細胞死が死んだ近位尿細管上皮細胞の比較的多数を占めている。ネクローシスにおいても，ミトコンドリアの役割が重要であり，ERKはネクローシスの抑制作用も有する[6]。

3．小胞体ストレスによる細胞死

小胞体ストレス自体はストレス応答の機構であるが，細胞毒が小胞体を標的としている場合，細胞死を誘導するシグナルが小胞体から送られ細胞死（アポトーシス，ネクローシス）を誘導することがある[7]。この一連の反応は，小胞体ストレスシグナリング経路によって制御されている。小胞体ストレスはミトコンドリア機能と深くかかわっ

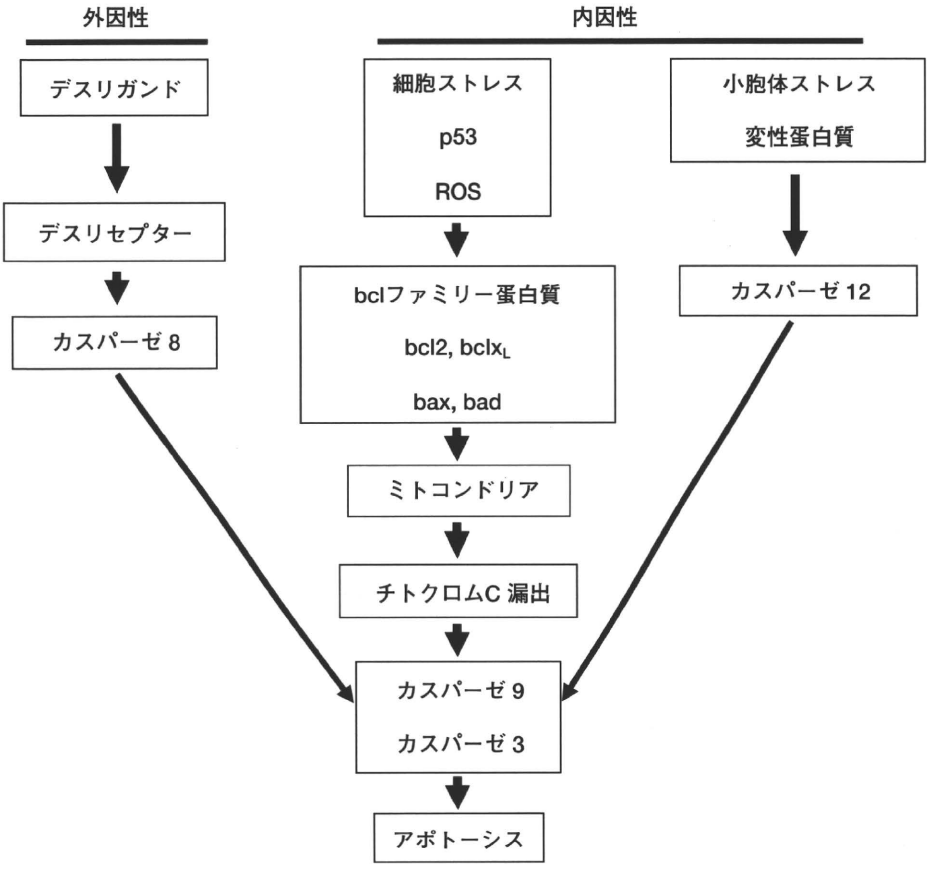

図1　アポトーシスシグナル伝達経路

ており，Bcl2 ファミリーの蛋白質の活性化による小胞体ストレスの誘導，引き続くカスパーゼ 12 そしてカスパーゼ 3 の活性化，さらに，小胞体ストレスシグナリングを制御する IRE1a への Bax や Bak の結合による JNK シグナル経路の活性化や，ほかの小胞体ストレス制御因子による転写因子 gadd153/CHOP10 の活性化などを介して細胞死を誘導する。

4．オートファジーによる細胞死

オートファジーは，アミノ酸の供給・再利用を重要な役割としており，ミトコンドリアなど細胞内器官の自食作用のために形成されるオートファーゴソームを特徴とする[3]。オートファジー自体は飢餓ストレスに対する応答機構であるが，細胞死を誘導する場合がある。最近の知見では，オートファジーはシスプラチンの腎毒性に対し防御作用があるといわれている[8,9]。

Ⅲ．腎毒性のある抗生物質と毒物

腎毒性と細胞毒性による細胞死シグナリングについて，2 つの細胞毒を例にとって述べよう（**図 2**）。まず腎毒性に特徴的なことは，近位尿細管上皮細胞の機能，すなわち細胞毒の濃縮的な細胞内蓄積，代謝，尿細管分泌，再吸収といったことである。腎毒性作用の場合，上皮細胞は細胞毒を濃縮することと，ミトコンドリアにおけるエネルギー代謝が活発なために毒性作用に対して感受性が高いことがあげられる[1]。こうした腎上皮細胞の分化した特徴と細胞死シグナリングは関係してくる。ここでは主に培養細胞を用いた研究成果からの知見をまとめる。

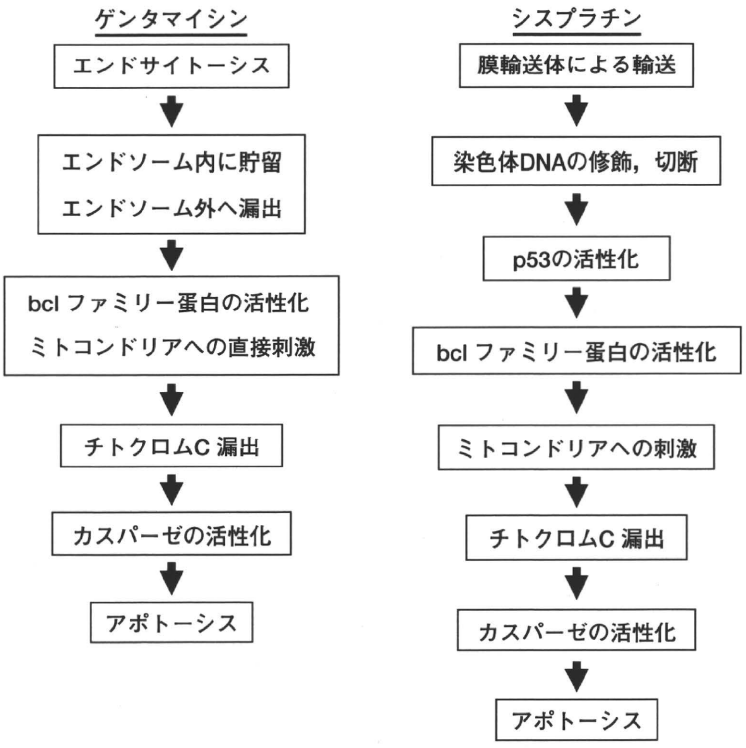

図2　ゲンタマイシンとシスプラチンの毒性シグナル伝達経路

1．ゲンタマイシン

エンドソームの飽和，ミトコンドリアの刺激と活性酸素の発生

ゲンタマイシンは近位尿細管上皮細胞の絨毛に発現している受容体メガリン（gp330）に結合し，エンドサイトーシスを介して細胞内に取り込まれ，エンドソームに蓄積される[1]。最終的にここから細胞質に流出されることによって毒性を惹起し，Bax の活性化，ミトコンドリアからのシトクロム C 漏出を経て，アポトーシスシグナリングを発生させる。またゲンタマイシンは細胞内の活性酸素生成も引き起こし，この経路からも細胞死に寄与している。

2．シスプラチン

DNA 損傷と p53 の活性化

シスプラチンは近位尿細管上皮細胞上の有機カチオントランスポータ（OCT2/SLC22A2）によって細胞内に取り込まれ，核内の染色体 DNA と共有結合し，最終的に DNA の切断を惹起する[10~12]。この DNA 損傷が p53 の活性化を誘導し，PUMA，PIDD といったアポトーシス促進因子の転写の誘導につながり，または直接 Bcl ファミリー蛋白質の活性化を引き起こして，ミトコンドリアの刺激，シトクロム C の漏出を介して，アポトーシスシグナリングの発生へと進行する。このメカニズムは，シスプラチンの抗癌薬としての作用と類似している[12]。シスプラチンの毒性には MAP キナーゼの活性化も重要な役割をもつ。JNK，p38 とともに通常は抗アポトーシス活性を示す ERK もこの場合アポトーシス促進に働く。細胞周期を制御する CDK2，p21 蛋白質や，アポトーシス促進因子である omi もシスプラチンによるアポトーシスメカニズムに重要とされる。シスプラチンは細胞内の活性酸素の生成も誘導し，この経路からも細胞死に寄与していると考えられている。小胞体もまたシスプラチン毒性の細胞内標的オルガネラであり，小胞体ストレス誘導によるアポトーシスにかかわっている[12]。

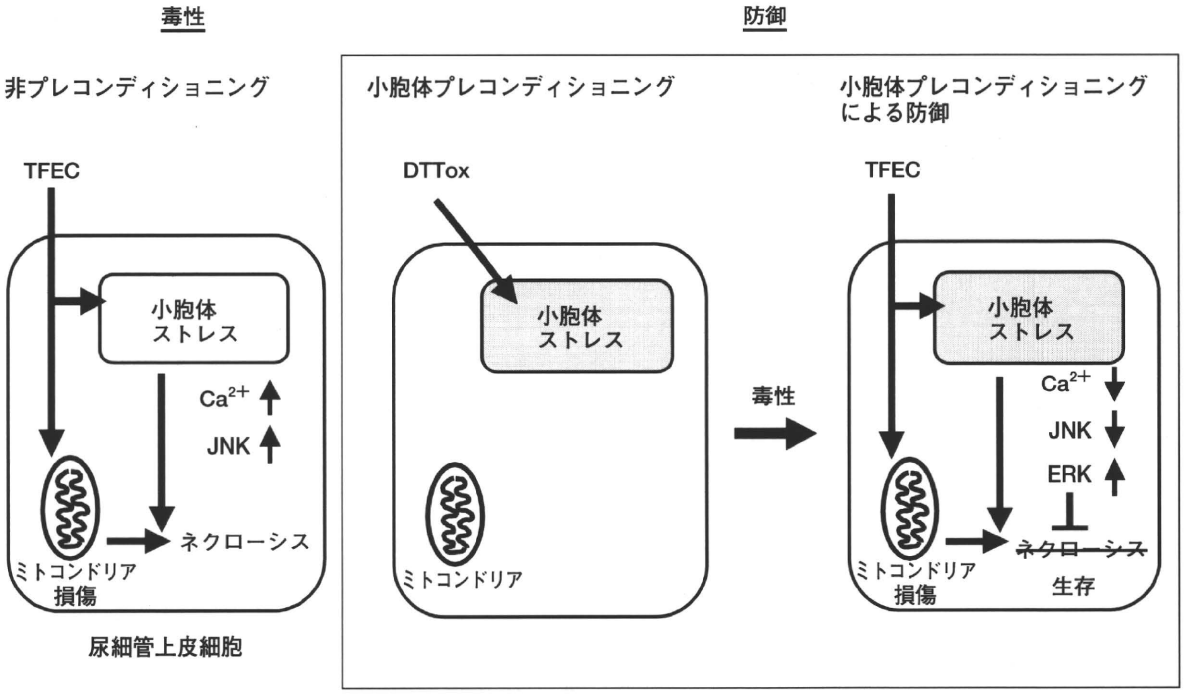

図3　小胞体プレコンディショニングによる細胞の毒物からの防御

IV. 細胞毒に対する防御能と細胞内シグナリングによる活性化

細胞は多様な細胞毒に対する防御能を備えており，それら発現を制御するシグナリング系が存在する。人為的にそれらのシグナリング系を活性化することによって毒性の発現や進行を阻害することができる。ここではいかにして防御するか，防御能獲得の方法について動物実験による研究成果を中心にまとめる。

防御の第1に，細胞毒取り込みの抑制があげられる。ゲンタマイシン誘発腎障害における受容体メガリンに対する競合が[13]，またシスプラチン腎症には，シスプラチンの細胞内取り込みを媒介するOCT2の阻害などの方法が検討されている[14]。次に，細胞内での毒性阻害，シスプラチンを例にとれば，カスパーゼの阻害，Bcl2の活性化，MAPキナーゼの阻害などがあげられる[12]。ゲンタマイシン毒性に対するプロスタサイクリンの防御能も知られている[15]。他方，細胞障害からの修復の促進も細胞毒性に対する防御機構の1つとしてあげられており，成長因子を中心に研究が行われている[1]。

最後にわれわれが行っている小胞体プレコンディショニングの研究について防御能獲得の方法の例として紹介する（**図3**）。われわれは腎毒性のあるシステインコンジュゲートTFECが小胞体ストレスを誘導し，小胞体シャペロンであるGRP78が発現することを発見した。そしてGRP78発現の阻害は細胞の感受性を高めることを確認した[16]。小胞体ストレスは本来，ストレス応答のメカニズム，防御反応であるため，穏やかな小胞体ストレスをあらかじめ誘導させることで，プレコンディショニングを起こし，致死量の細胞毒刺激に対する防御能獲得を実現した[16~18]。このメカニズムは，細胞内カルシウム濃度，ERKの活性化，JNK阻害であることが一部わかっている[6]。この小胞体プレコンディショニングはラットを使った動物実験でも再現できることが示されている[19]。

まとめ

抗生物質や細胞毒による細胞死は，細胞内シグナリングによって制御されている。この細胞内シグナリングにはさまざまなレベルがあり，最終的に細胞死を引き起こす。そして毒性による細胞死の細胞内シグナリングを理解することは，細胞毒性による細胞死に対する防御戦略を考えるうえで重要性が高い。

文　献

1) Servais H, Ortiz A, Devuyst O, et al：Renal cell apoptosis induced by nephrotoxic drugs：cellular and molecular mechanisms and potential approaches to modulation. Apoptosis **13**：11-32, 2008
2) van de Water B, de Graauw M, Le Devedec S, et al：Cellular stress responses and molecular mechanisms of nephrotoxicity. Toxicol Lett **162**：83-93, 2006
3) Degterev A, Yuan J：Expansion and evolution of cell death programmes. Nat Rev Mol Cell Biol **9**：378-390, 2008
4) Junttila MR, Li SP, Westermarck J：Phosphatase-mediated crosstalk between MAPK signaling pathways in the regulation of cell survival. Faseb J **22**：954-965, 2008
5) Golstein P, Kroemer G：Cell death by necrosis：towards a molecular definition. Trends Biochem Sci **32**：37-43, 2007
6) Hung CC, Ichimura T, Stevens JL, et al：Protection of renal epithelial cells against oxidative injury by endoplasmic reticulum stress preconditioning is mediated by ERK1/2 activation. J Biol Chem **278**：29317-29326, 2003
7) Kitamura M：Endoplasmic reticulum stress and unfolded protein response in renal pathophysiology：Janus faces. Am J Physiol Renal Physiol **295**：F323-334, 2008
8) Periyasamy-Thandavan S, Jiang M, Wei Q, et al：Autophagy is cytoprotective during cisplatin injury of renal proximal tubular cells. Kidney Int **74**：631-640, 2008
9) Yang C, Kaushal V, Shah SV, et al：Autophagy is associated with apoptosis in cisplatin injury to renal tubular epithelial cells. Am J Physiol Renal Physiol **294**：F777-787, 2008
10) Yonezawa A, Masuda S, Nishihara K, et al：Association between tubular toxicity of cisplatin and expression of organic cation transporter rOCT2 (Slc22a2) in the rat. Biochem Pharmacol **70**：1823-1831, 2005
11) Yokoo S, Yonezawa A, Masuda S, et al：Differential contribution of organic cation transporters, OCT2 and MATE1, in platinum agent-induced nephrotoxicity. Biochem Pharmacol **74**：477-487, 2007
12) Pabla N, Dong Z：Cisplatin nephrotoxicity：mechanisms and renoprotective strategies. Kidney Int **73**：994-1007, 2008
13) Nagai J, Saito M, Adachi Y, et al：Inhibition of gentamicin binding to rat renal brush-border membrane by megalin ligands and basic peptides. J Control Release **112**：43-50, 2006
14) Tanihara Y, Masuda S, Katsura T, et al：Protective effect of concomitant administration of imatinib on cisplatin-induced nephrotoxicity focusing on renal organic cation transporter OCT2. Biochem Pharmacology 2009, doi：10. 1016/j. bcp. 2009. 06. 014
15) Hsu YH, Chen CH, Hou CC, et al：Prostacyclin protects renal tubular cells from gentamicin-induced apoptosis via a PPARalpha-dependent pathway. Kidney Int **73**：578-587, 2008
16) Liu H, Bowes RC 3rd, van de Water B, et al：Endoplasmic reticulum chaperones GRP78 and calreticulin prevent oxidative stress, Ca^{2+} disturbances, and cell death in renal epithelial cells. J Biol Chem **272**：21751-21759, 1997
17) Halleck MM, Liu H, North J, et al：Reduction of trans-4,5-dihydroxy-1,2-dithiane by cellular oxidoreductases activates gadd153/chop and grp78 transcription and induces cellular tolerance in kidney epithelial cells. J Biol Chem **272**：21760-21766, 1997
18) Liu H, Miller E, van de Water B, et al：Endoplasmic reticulum stress proteins block oxidant-induced Ca^{2+} increases and cell death. J Biol Chem **273**：12858-12862, 1998
19) Asmellash S, Stevens JL, Ichimura T：Modulating the endoplasmic reticulum stress response with trans-4,5-dihydroxy-1,2-dithiane prevents chemically induced renal injury *in vivo*. Toxicol Sci **88**：576-584, 2005

*　　*　　*

Biochemical Pharmacology 77 (2009) 1429–1436

Contents lists available at ScienceDirect

Biochemical Pharmacology

journal homepage: www.elsevier.com/locate/biochempharm

Transport of guanidine compounds by human organic cation transporters, hOCT1 and hOCT2

Naoko Kimura, Satohiro Masuda, Toshiya Katsura, Ken-ichi Inui *

Department of Pharmacy, Kyoto University Hospital, Faculty of Medicine, Kyoto University, Sakyo-ku, Kyoto 606-8507, Japan

ARTICLE INFO

Article history:
Received 28 November 2008
Accepted 16 January 2009

Keywords:
Guanidine
Aminoguanidine
OCT1
OCT2
Uremic toxins
Kidney

ABSTRACT

Although some guanidine compounds were reported as superior substrates for organic cation transporter (OCT)2 than OCT1, it was unclear whether this guanidino group was an important factor in determining the specificity of hOCT1 and hOCT2. Using HEK293 cells transfected with human (h)OCT1 or hOCT2 cDNA, we assessed the role of hOCT1 and/or hOCT2 in the transport of guanidine compounds such as uremic toxins and therapeutic agents. Guanidine, creatinine and aminoguanidine more markedly inhibited the uptake of [^{14}C]tetraethylammonium (TEA) by hOCT2 than by hOCT1. [^{14}C]TEA uptake by hOCT2, but not hOCT1, was *trans*-stimulated by unlabeled guanidine, methylguanidine, creatinine, aminoguanidine and phenylguanidine. In patients with renal failure, the impairment of hOCT2 might decrease the excretion of guanidine, methylguanidine, and creatinine as uremic toxins. The uptake of aminoguanidine, a candidate for an anti-diabetic agent, was enhanced by hOCT2 with the Michaelis constant (K_m) of 4.10 ± 0.35 mM. Metformin, which was also an anti-diabetic agent, and creatinine more potently inhibited the uptake of [^{14}C]aminoguanidine by hOCT2 than that by hOCT1. Aminoguanidine had little impact on the uptake of [^{14}C]metformin by hOCT1, but inhibited that by hOCT2 with the IC_{50} of 1.49 ± 0.14 mM. These results indicated that the specificity of hOCT1 and hOCT2 was not determined simply by guanidino group. Among guanidine compounds, aminoguanidine was identified as a new superior substrate for hOCT2.

1. Introduction

Organic cation transporters (OCTs) play an important role in the tissue distribution of a wide variety of positively charged molecules, including drugs and endogenous substrates. Human organic cation transporter 1 (hOCT1) is preferentially expressed in the liver, and mediates hepatic uptake of cationic compounds [1,2]. In contrast, hOCT2 is specifically expressed in the renal proximal tubules, and is considered to mediate the renal uptake of cationic compounds [3,4]. Functional studies suggested that these transporters were often similar in substrate specificity [4,5], but in recent years, the compounds with a guanidino group such as guanidine, creatinine, and metformin were reported to be better substrates for OCT2 than OCT1 in rat and/or human [6–8]. However, it was unclear whether a guanidino group was important in determining the affinity of the two transporters.

Some guanidine compounds have been known as uremic toxins [9–14]. Other guanidine compounds have been reported as anti-diabetic agents, in particular, aminoguanidine is positively charged at physiological pH, and its renal clearance was more than twice the glomerular filtration rate (GFR), suggesting the contribution of tubular secretion [15–17].

The aim of this study was to compare the specificity of hOCT1 and hOCT2 for several guanidine compounds, including uremic toxins and aminoguanidine (Fig. 1).

2. Materials and methods

2.1. Materials

[Ethyl-1-^{14}C]tetraethylammonium bromide (55 mCi/mmol) was purchased from American Radiolabeled Chemicals (St. Louis, MO, USA). [^{14}C]aminoguanidine (51 mCi/mmol) and [biguanidine-^{14}C]metformin hydrochloride (26 mCi/mmol) were purchased from Moravek Biochemicals, Inc. (Brea, CA). [^{3}H]1-methyl-4-phenylpyridium acetate (MPP) (2.7 TBq/mmol) was purchased from PerkinElmer Life and Analytical Sciences Waltham, MA). Creatinine and guanidine hydrochloride were obtained from Nacalai Tesque (Kyoto, Japan). N_{α}-Acetyl-L-arginine, aminoguanidine bicarbonate salt, 1-butylguanidine sulfate, creatine anhydrous, 1,1-dimethylguanidine sulfate salt, guanidinoacetic acid, guanidinosuccinic acid, guanidinovaleric acid hemihydrate, methylguanidine hydrochloride, N-propylguanidine sulfate, phenylguanidine carbonate salt, 1,1,3,3-tetramethylguanidine, and 1-

* Corresponding author. Tel.: +81 75 751 3577; fax: +81 75 751 4207.
E-mail address: inui@kuhp.kyoto-u.ac.jp (K.-i. Inui).

0006-2952/$ – see front matter © 2009 Elsevier Inc. All rights reserved.
doi:10.1016/j.bcp.2009.01.010

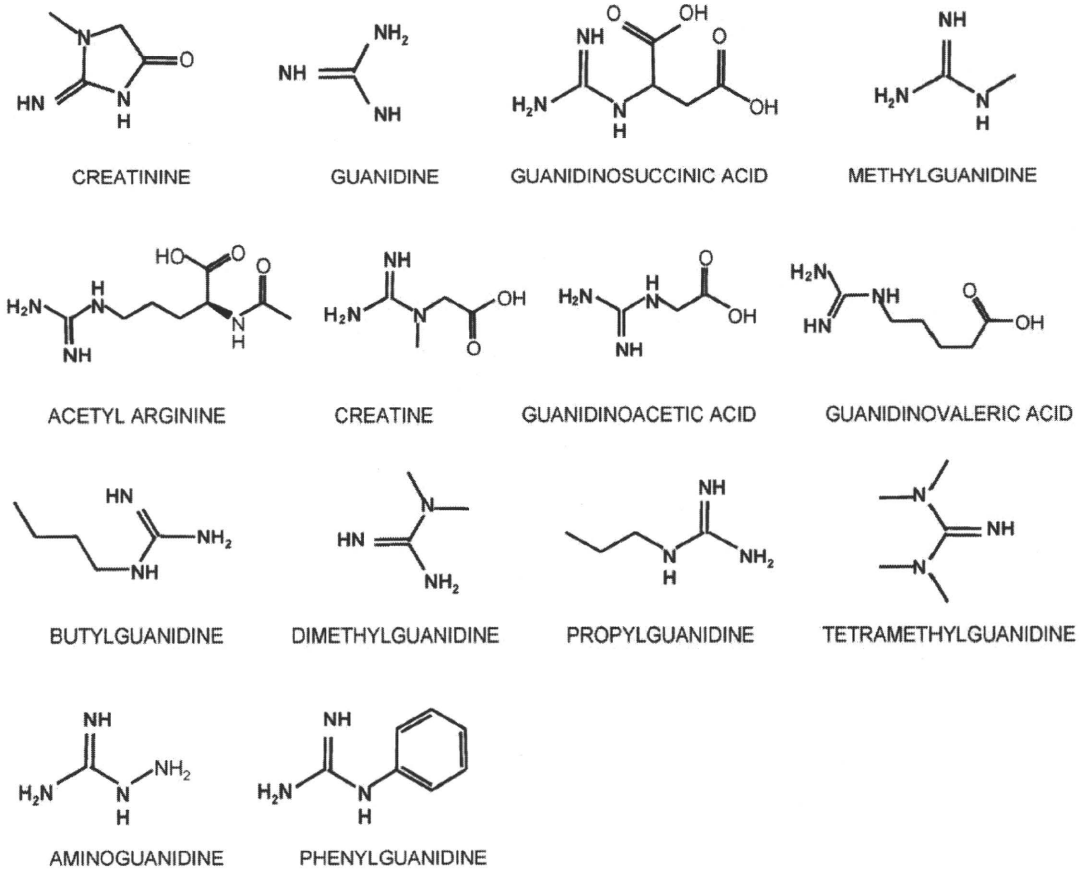

Fig. 1. Chemical structures of guanidine compounds.

methyl-4-phenylpyridium iodide were purchased from Sigma–Aldrich Co. (St. Louis, MO, USA). All other compounds used were of the highest purity available.

2.2. Cell culture

HEK 293 cells (ATCC CRL-1573, American Type Culture Collection, Manassas, VA) were cultured in complete medium consisting of Dulbecco's modified Eagle's medium with 10% fetal bovine serum in an atmosphere of 5% CO_2/95% air at 37 °C, and used as host cells. The transfectant stably expressing hOCT1 and hOCT2 were established as described previously [7,8]. The HEK293 cells transiently transfected with pCMV6-XL4 plasmid vector DNA (OriGene Technologies, Rockville, MD) containing hOCT1, hOCT2 or hOCT3-cDNA were prepared as described previously [7,18]. The cell monolayers were used at day 3 of culture for uptake experiments. In the present study, cells were used between the 78th and 90th passages.

2.3. Uptake experiments

The cellular uptake of cationic compounds was measured with monolayer cultures of HEK293 cells grown on poly-D-lysine-coated 24-well plates [7,19]. The protein content of the solubilized cells was determined by the method of Bradford [20], using a Bio-Rad Protein Assay Kit (Bio-Rad Laboratories, Hercules, CA) with bovine-globulin as a standard. For the *cis*-inhibition study, the uptake of [^{14}C]tetraethylammonium (TEA), [^{14}C]aminoguanidine, or [^{14}C]metformin was achieved by adding various concentrations of unlabeled inhibitors to the incubation medium. IC_{50} values were calculated from the inhibition plots based on the equation, $V = V_0/[1 + ([I]/IC_{50})^n]$, by a nonlinear least square regression analysis with Kaleidagraph Version 4.00 (Synergy Software, Reading, PA, USA). V and V_0 were the uptake rates of [^{14}C]TEA, [^{14}C]aminoguanidine, or [^{14}C]metformin in the presence and absence of inhibitor, respectively. [I] is the concentration of inhibitor, and n is the Hill coefficient. For the

Table 1
The apparent IC_{50} values of guanidine compounds for [^{14}C]TEA uptake by hOCT1 and hOCT2.

Guanidine compounds	IC_{50} values for [^{14}C]TEA uptake (mM)	
	hOCT1	hOCT2
Uremic toxins[a]		
Creatinine	N/A	6.06 ± 0.98
Guanidine	N/A	3.03 ± 0.42
Guanidinosuccinic acid	1.54 ± 0.15	1.47 ± 0.20
Methylguanidine	2.36 ± 0.06	1.53 ± 0.31
Acetyl arginine	N/A	N/A
Creatine	N/A	N/A
Guanidinoacetic acid	N/A	N/A
Guanidinovaleric acid	0.66 ± 0.03	1.18 ± 0.14*
Butylguanidine	0.21 ± 0.02	0.12 ± 0.01*
Dimethylguanidine	0.54 ± 0.09	0.36 ± 0.02
Propylguanidine	0.36 ± 0.04	0.29 ± 0.02
Tetramethylguanidine	0.48 ± 0.08	0.78 ± 0.13
Aminoguanidine	N/A	0.80 ± 0.11
Phenylguanidine	0.23 ± 0.03	0.26 ± 0.02

See experimental conditions in the legend of Fig. 2. The apparent IC_{50} values were calculated from inhibition plots (Fig. 2) by nonlinear regression analysis as described in Section 2. The data represent the mean ± S.E. of three independent experiments. N/A, not available. *$P < 0.05$, significantly different from the IC_{50} value of hOCT1.

[a] [18].

trans-inhibition study, the cells were preincubated with either the incubation medium (control) or the incubation medium plus the indicated concentration of unlabeled compounds for 30 min. The cells were rinsed twice with 1 mL of ice-cold incubation medium before the uptake experiments. The concentration dependence of the transport of aminoguanidine by hOCT1 and hOCT2 was analyzed using the Michaelis–Menten equation; $V = V_{max} \cdot [S] / (K_m + [S]) + K_{diff} \cdot [S]$, where V is the transport rate, V_{max} is the maximum transport rate, [S] is the concentration of aminoguanidine, K_m is the Michaelis constant and K_{diff} is a diffusion constant. The accumulation of [^{14}C]aminoguanidine by hOCT1- and hOCT2-HEK293 cells was measured at various concentrations (0.1–10 mM) for 2 min at 37 °C (pH 7.4).

2.4. Statistical analysis

Data were expressed as the mean ± S.E. Data were analyzed statistically using the non-paired Student's *t* test or one-way analysis of variance (ANOVA) and Dunnett's multiple comparison procedure.

3. Results

3.1. Inhibitory effects of guanidine compounds on TEA uptake by hOCT1 and hOCT2

To compare the specificity of hOCT1 and hOCT2, the inhibitory effects of several guanidine compounds on the uptake of [^{14}C]TEA

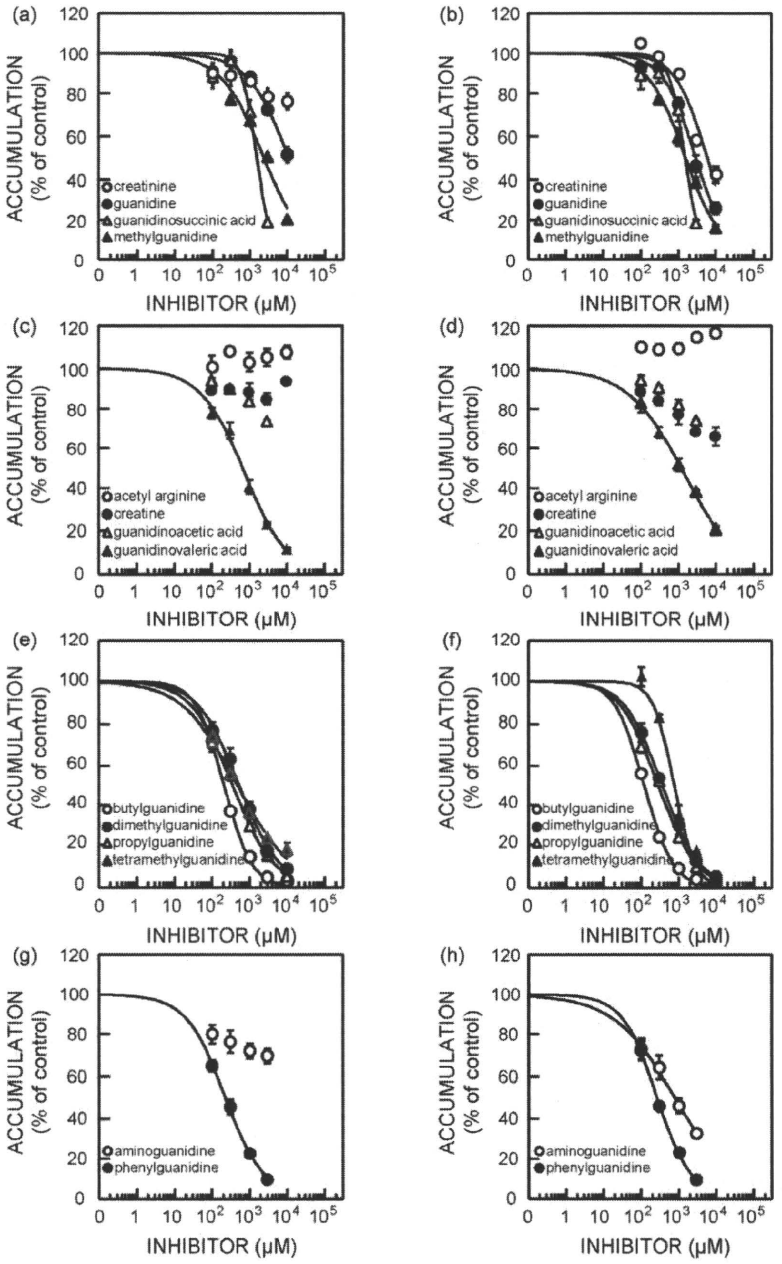

Fig. 2. Effects of guanidine compounds on [^{14}C]TEA uptake by hOCT1 (a, c, e and g) and hOCT2 (b, d, f and h). HEK293 cells transfected with hOCT1 and hOCT2 were incubated at 37 °C for 2 min with 5 μM [^{14}C]TEA (pH 7.4) in the presence of (a and b); creatinine (open circle), guanidine (closed circle), guanidinosuccinic acid (open triangle), or methylguanidine (closed triangle), (c and d); acetyl arginine (open circle), creatine (closed circle), guanidinoacetic acid (open triangle), or guanidinovaleric acid (closed triangle), (e and f); butylguanidine (open circle), dimethylguanidine (closed circle), propylguanidine (open triangle), or tetramethylguanidine (closed triangle), (g and h); aminoguanidine (open circle), or phenylguanidine (closed circle). Each point represents the mean ± S.E. of three independent experiments.

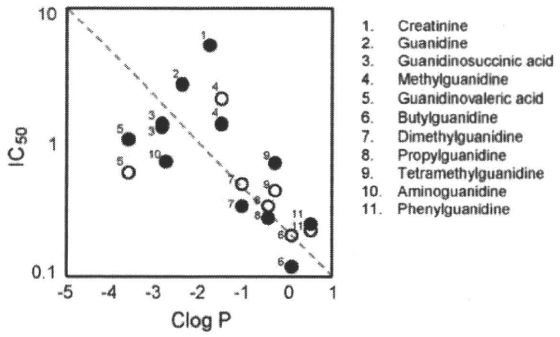

Fig. 3. Relationship between the calculated hydrophobicity (*C* log *P*) of guanidine compounds and IC_{50} values for inhibition of [^{14}C]TEA uptake by hOCT1 and hOCT2. The relationship between the calculated hydrophobicity (*C* log *P*) of guanidine compounds and the measured IC_{50} values for inhibition of [^{14}C]TEA uptake in hOCT1-HEK293 (open circle) and hOCT2-HEK293 (closed circle) cells. See experimental conditions in the legend of Fig. 2. The apparent IC_{50} values were calculated from inhibition plots (Fig. 2) by nonlinear regression analysis as described in Section 2. Octanol/water partition coefficients (log *P*) were calculated using Chem Draw Ultra 7.0 software.

(a typical substrate for the organic cation transporter) were examined (Table 1, Fig. 2). The inhibitory effects of guanidinosuccinic acid and methylguanidine were comparable between hOCT1 and hOCT2. Guanidine and creatinine had stronger inhibitory effects on [^{14}C]TEA uptake by hOCT2 than by hOCT1, whereas guanidinovaleric acid inhibited hOCT1 more than hOCT2. Guanidinoacetic acid tended to inhibit the uptake of [^{14}C]TEA by both hOCT1 and hOCT2, while creatine tended only to inhibit the hOCT2. Acetyl arginine did not inhibit [^{14}C]TEA uptake by either transporters. The inhibition curves of alkyl guanidine compounds for [^{14}C]TEA uptake showed that alkyl guanidine compounds had potent inhibitory effects on both hOCT1 and hOCT2, and that only butylguanidine had moderately higher affinity for hOCT2 than hOCT1. Phenylguanidine had an inhibitory effect on [^{14}C]TEA uptake by both hOCT1 and hOCT2, while aminoguanidine had a much greater inhibitory effect on hOCT2 than hOCT1. Fig. 3 plots the relationship between the log of the measured IC_{50} values (Table 1) and the calculated log *P* values (*C* log *P*) of guanidine compounds.

3.2. *Trans*-stimulation effects of guanidine compounds on TEA uptake by hOCT1 and hOCT2

To examine whether these guanidine compounds were substrates of hOCT1 and hOCT2, *trans*-stimulation experiments were performed. The transfectants were preincubated with a concentration equivalent to approximately 3-fold the IC_{50} value of the unlabeled guanidine compounds, or else with 10 mM if the IC_{50} value was not available (Table 1) [5]. Then, the [^{14}C]TEA uptake by the preincubated transfectants was measured. Fig. 4 shows the

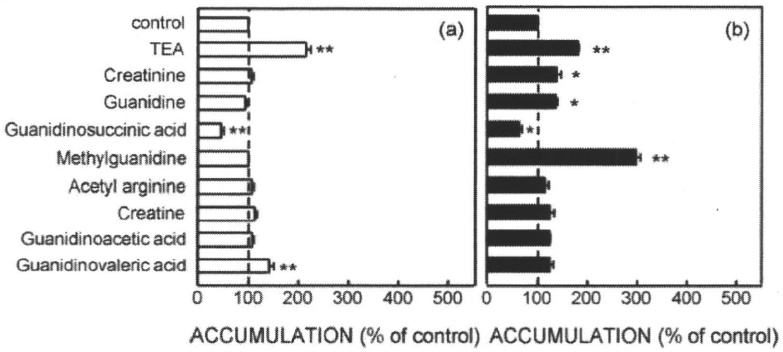

Fig. 4. *Trans*-stimulation effects of guanidine compounds as uremic toxins on [^{14}C]TEA uptake by hOCT1 (a) and hOCT2 (b). HEK-hOCT1 and HEK-hOCT2 cells were incubated for 2 min at 37 °C with 5 μM [^{14}C]TEA after preincubation with incubation medium (control) or incubation medium containing TEA (5 mM), creatinine (10 mM, hOCT1; 20 mM, hOCT2), guanidine (10 mM, hOCT1; 9 mM, hOCT2), guanidinosuccinic acid (5 mM, hOCT1; 4 mM, hOCT2), methylguanidine (7 mM hOCT1; 5 mM, hOCT2), acetyl arginine (10 mM), creatine (10 mM), guanidinoacetic acid (10 mM), and guanidinovaleric acid (2 mM, hOCT1; 4 mM, hOCT2) for 30 min at 37 °C, respectively. Data are expressed as a percentage of the control value. Control values for HEK-hOCT1 and HEK-hOCT2 were 25.6 ± 1.4 and 14.5 ± 1.2 pmol/mg protein/2 min, respectively. Each column represents the mean ± S.E. of three independent experiments. $^{*}P < 0.05$, $^{**}P < 0.01$, significantly different from the control.

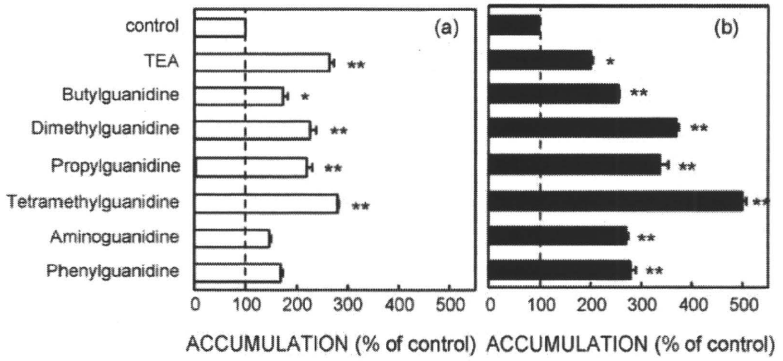

Fig. 5. *Trans*-stimulation effects of alkyl guanidine compounds, aminoguanidine and phenylguanidine on [^{14}C]TEA uptake by hOCT1 (a) and hOCT2 (b). HEK-hOCT1 and HEK-hOCT2 cells were incubated for 2 min at 37 °C with 5 μM [^{14}C]TEA after preincubation with incubation medium (control) or incubation medium containing TEA (5 mM), butylguanidine (0.6 mM, hOCT1; 0.4 mM, hOCT2), dimethylguanidine (2 mM hOCT1; 1 mM, hOCT2), propylguanidine (1 mM, hOCT1; 0.9 mM, hOCT2), tetramethylguanidine (1 mM, hOCT1; 2 mM, hOCT2), aminoguanidine (10 mM, hOCT1; 2 mM hOCT2) and phenylguanidine (0.7 mM, hOCT1; 0.8 mM, hOCT2) for 30 min at 37 °C, respectively. Data are expressed as a percentage of the control value. Control values for HEK-hOCT1 and HEK-hOCT2 were 25.9 ± 1.4 and 11.0 ± 0.2 pmol/mg protein/2 min, respectively. Each column represents the mean ± S.E. of three independent experiments. $^{*}P < 0.05$, $^{**}P < 0.01$, significantly different from the control.

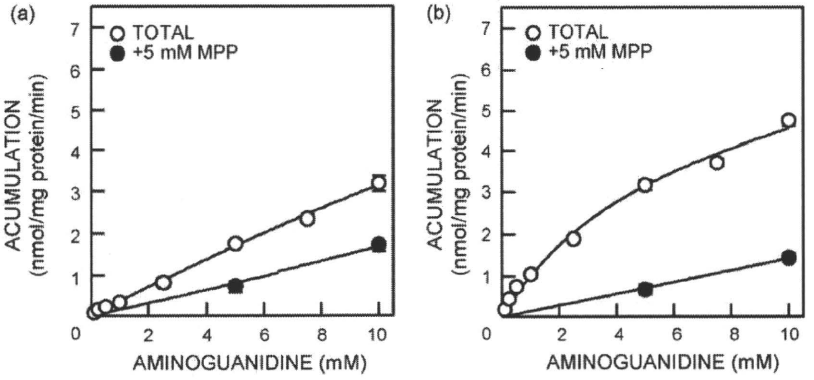

Fig. 6. Concentration dependence of [^{14}C]aminoguanidine transport by hOCT1 (a) and hOCT2 (b). hOCT1 and hOCT2 transfectants were incubated at 37 °C for 2 min with various concentrations of [^{14}C]aminoguanidine (0.1, 0.25, 0.5, 1, 2.5, 5, 7.5 and 10 mM) in the absence (open circle) or presence (closed circle) of 5 mM 1-methyl-4-phenylpyridinium (pH 7.4). Each point represents the mean ± S.E. of three independent experiments.

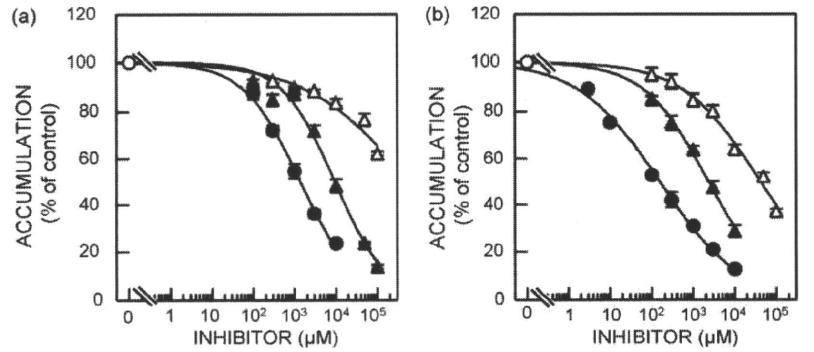

Fig. 7. Effects of TEA, creatinine and metformin on [^{14}C]aminoguanidine transport by hOCT1 (a) and hOCT2 (b). HEK 293 cells transfected with hOCT1 and hOCT2 were incubated at 37 °C for 2 min with 10 μM [^{14}C]aminoguanidine (pH 7.4) in the absence (open circle) or presence of TEA (closed circle), creatinine (open triangle), or metformin (closed triangle). Each point represents the mean ± S.E. of three independent experiments.

trans-stimulation effects of endogenous guanidine compounds as uremic toxin. Preincubation with unlabeled guanidine, methylguanidine, and creatinine significantly increased the uptake of [^{14}C]TEA by hOCT2 but not hOCT1. Meanwhile, preincubation with guanidinovaleric acid increased the [^{14}C]TEA uptake by hOCT1 but not hOCT2. As shown in Fig. 5, we examined the *trans*-stimulation effects of the other guanidine compounds. Preincubation with unlabeled butylguanidine, propylguanidine, dimethylguanidine, and tetramethylguanidine increased the uptake of [^{14}C]TEA by both transfectants. On the other hand, the preincubation with aminoguanidine and phenylguanidine significantly enhanced the [^{14}C]TEA uptake by hOCT2 but not hOCT1.

3.3. Uptake of aminoguanidine by hOCT1 and hOCT2

To obtain more information about the substrate specificity of hOCT2, the transport characteristics of [^{14}C]aminoguanidine was compared between hOCT1 and hOCT2. Fig. 6 shows the concentration dependence of [^{14}C]aminoguanidine uptake by hOCT1 and hOCT2. The uptake by hOCT2 was greater than that by hOCT1. The uptake was saturated at high concentrations in hOCT2-expressing cells, although no such saturation was observed in hOCT1-expressing cells. The apparent Michaelis–Menten constant (K_m) for the uptake of [^{14}C]aminoguanidine by hOCT2 was 4.10 ± 0.35 mM. The maximal uptake rate (V_{max}) in hOCT2-expressing cells was 4.40 ± 0.42 nmol/mg protein/min (mean ± S.E. of three separate experiments). Next, we examined the inhibitory effects of TEA, creatinine and metformin on the uptake of [^{14}C]aminoguanidine by hOCT1 and hOCT2 (Fig. 7). Fig. 7a and b shows the inhibition curves of TEA, creatinine and metformin in hOCT1- and hOCT2-expressing cells, respectively. Although TEA, creatinine and metformin inhibited the uptake of [^{14}C]aminoguanidine by both hOCT1 and hOCT2 in a dose-dependent manner, the uptake by hOCT2 was more inhibited. We calculated the IC_{50} values of these cationic compounds from the inhibition plots as described in Section 2 (Table 2). We also examined the inhibitory effect of aminoguanidine on the uptake of [^{14}C]metformin (Fig. 8). Aminoguanidine had little impact on the uptake of [^{14}C]metformin by hOCT1, and the IC_{50} value of aminoguanidine was not estimated (Fig. 8a). However, aminoguanidine inhibited the [^{14}C]metformin uptake by hOCT2 with the IC_{50} of 1.49 ± 0.14 mM (Fig. 8b).

To confirm aminoguanidine as a new substrate selective for hOCT2, the influence of *cis*-inhibition and *trans*-stimulation of aminoguanidine on the [^{3}H]MPP transport by hOCT3 was

Table 2
The apparent IC_{50} values of cationic compounds for [^{14}C]aminoguanidine uptake by hOCT1 and hOCT2.

Inhibitors	IC_{50} values for [^{14}C]aminoguanidine uptake (mM)	
	hOCT1	hOCT2
TEA	1.39 ± 0.06	0.16 ± 0.02
Creatinine	N/A	42.4 ± 2.6
Metformine	9.48 ± 0.56	2.37 ± 0.20

See experimental conditions in the legend of Fig. 7. The apparent IC_{50} values were calculated from inhibition plots (Fig. 7) by nonlinear regression analysis as described in Section 2. The data represent the mean ± S.E. of three independent experiments. N/A, not available.

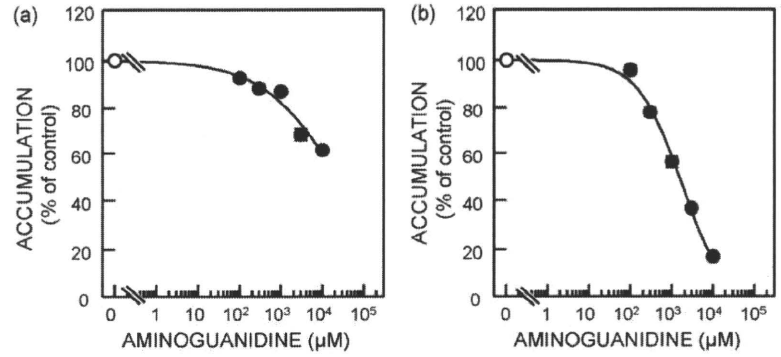

Fig. 8. Effects of aminoguanidine on [^{14}C]metformin transport by hOCT1 (a) and hOCT2 (b). HEK 293 cells transfected with hOCT1 and hOCT2 were incubated at 37 °C for 2 min with 10 μM [^{14}C]metformin (pH 7.4) in the absence (open circle) or presence of aminoguanidine (closed circle). Each point represents the mean ± S.E. of three independent experiments.

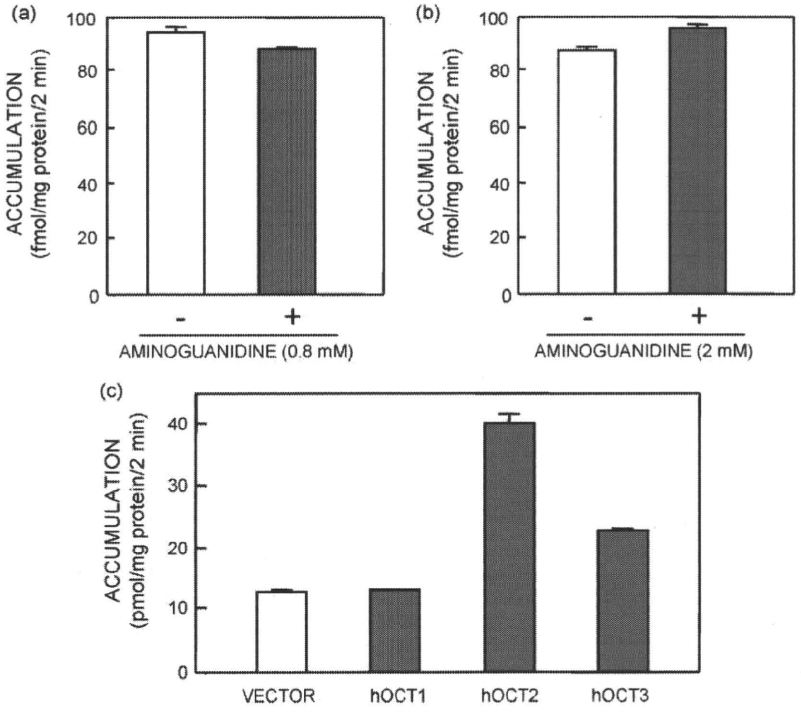

Fig. 9. Influence of *cis*-inhibition (a) and *trans*-stimulation (b) of aminoguanidine on the [^{3}H]MPP transport by hOCT3, and [^{14}C]aminoguanidine transport by hOCT1, hOCT2 and hOCT3 (c). (a) HEK293 cells transiently expressing hOCT3 were incubated at 37 °C for 2 min with 13.7 nM [^{3}C]MPP (pH 7.4) in the absence (−) or presence (+) of aminoguanidine (0.8 mM). (b) HEK293 cells transiently expressing hOCT3 were incubated for 2 min at 37 °C with 13.7 nM [^{3}H]MPP after preincubation with incubation medium (−) or incubation medium containing aminoguanidine (2 mM) (+) for 30 min at 37 °C. (c) HEK293 cells transfected with empty vector, hOCT1, hOCT2 or hOCT3 were incubated for 2 min at 37 °C with 5 μM [^{14}C]aminoguanidine (pH 7.4). Each column represents the mean ± S.E. of three monolayers.

examined in comparison with hOCT2 (Fig. 9a and b). The hOCT3-mediated uptake of [^{3}H]MPP was little affected by aminoguanidine in both conditions of *cis*-inhibition and *trans*-stimulation. In addition, the transport of [^{14}C]aminoguanidine by hOCT2 was the highest among three OCT isoforms (Fig. 9c).

4. Discussion

Previous reports suggested that guanidine and creatinine, which had a guadinino group, were predominantly transported by OCT2 rather than OCT1 [6,7]. We tested the hypothesis that the guanidino group was a decisive factor in being recognized by hOCT2, but could not found such selectivity simply by this group. At the same time, we discovered that aminoguanidine was a new superior substrate for hOCT2 than hOCT1.

Several guanidine compounds were reported to accumulate in blood with renal insufficiency, some being described as uremic toxins [9–14]. Guanidinosuccinic acid and methylguanidine had the two highest scores for the uremic concentration (C_U)/normal concentration (C_N) ratio, and there were also significant differences between the C_U and C_N of guanidine and creatinine [14]. The plasma concentrations of many cationic drugs increase with renal failure. It has been considered that the tubular secretion of organic cations is impaired and the elevated plasma level of alpha1 acid glycoprotein prevents the renal excretion in renal failure [21–25]. Based on the present results, it is also possible that the uremic guanidine compounds inhibit the excretion of cationic drugs mediated by hOCT.

Fig. 3 shows the relationship between the inhibitory patterns and the *C* log *P* values of guanidine compounds. In guanidine

compounds, hydrophobicity was not the major factor in determining the affinity for hOCT as it was, for example, in n-tetraalkylammonium [5,26,27].

In the *trans*-stimulation study, we showed that the [^{14}C]TEA uptake by hOCT2, but not hOCT1, were increased by preincubation with unlabeled guanidine, methylguanidine, creatinine, aminoguanidine and phenylguanidine. Possibly, these compounds are transported by hOCT2 and the dysfunction of hOCT2 with renal failure decreases the excretion of guanidine, methylguanidine, and creatinine as uremic toxins.

Because the three uremic guanidine compounds, guanidinosuccinic acid, methylguanidine and guanidinovaleric acid inhibited [^{14}C]TEA uptake by hOCT1 as well as hOCT2, the pharmacokinetics of the cationic drugs may be affected in the patients with renal failure. The [^{14}C]TEA uptake by hOCT1 was *trans*-stimulated by guanidinovaleric acid, suggesting the hOCT1-mediated transport of guanidinovaleric acid compensating the impaired renal function. It might relate to the fact that the serum level of guanidinovaleric acid in the patients with renal insufficiency was similar to normal values [10,13].

Among 14 guanidine compounds, aminoguanidine was found to be a selective substrate for hOCT2 compared to hOCT1 and hOCT3. A guanidine compound agmatine (1-amino-4-guanidobutane) was reported as a substrate for hOCT2 and hOCT3, but not for hOCT1 [28], while guanidine was transported by rOCT2, but not by rOCT1 and hOCT3 [6]. Therefore, aminoguanidine as well as agmatin and guanidine can be a good probe to examine the transport activity of hOCT2 in comparison with hOCT1 and hOCT3.

The apparent affinity of aminoguanidine for hOCT2 was similar to that of creatinine (K_m = 4.0 mM) [7] and lower than that of metformin (K_m = 1.4 mM) [19]. Aminoguanidine, which inhibits many diabetes-related complications, remains under therapeutic testing [16,17,29]. Because aminoguanidine was excreted into urine by tubular secretion as well as glomerular filtration and hOCT2 was the most abundant organic cation transporter in the basolateral membranes of human kidney [3,15], the secretion of aminoguanidine may be predominantly mediated by hOCT2.

In ACTION I trial (*A* Clinical *T*rial *I*n *O*vert *N*ephropathy of Type *1* Diabetics), which included patients with type 1 diabetes mellitus [17], aminoguanidine reduced significantly secondary measures of outcome such as proteinuria and had additional effects on diabetic retinopathy and circulating lipid levels. However, the reduction in the primary end point of time to doubling of the serum creatinine concentration was not statistically significant. Although creatinine clearance is often used for the estimation of GFR, creatinine is also excreted via tubular secretion mediated by hOCT2 [7,30,31]. Aminoguanidine might inhibit the transport of creatinine by hOCT2 and increase the serum concentration of creatinine without inducing renal impairment. Therefore, the other parameters whose elimination was unaffected by aminoguanidine should have been used.

Although creatinine and metformin were also excreted into urine through transport by hOCT2 [7,19], their IC_{50} values for aminoguanidine uptake by hOCT2 (creatinine, 42.4 mM; metformin, 2.37 mM) were much higher than the physiological concentrations of creatinine (about 45–85 μM for male and 30–60 μM for female) and metformin (about 15–25 μM) (Table 2, Fig. 7) [24,32–34]. Therefore, the transport of aminoguanidine mediated by hOCT2 is not likely to be affected by creatinine and metformin, and diabetic patients whose plasma creatinine concentrations are increased or who use metformin may be able to use aminoguanidine safely. It was reported that the maximum aminoguanidine concentration was only 40 μM, during the interdialytic period [15]. It is also probable that aminoguanidine has little effect on the transport of metformin mediated by hOCT2, at the physiological concentrations (Fig. 8).

In this study, we demonstrated that many guanidine compounds examined had relatively equal affinity to hOCT1 and hOCT2 and could not found the selectivity for hOCT2 simply by guanidino group. Among guanidine compounds, we newly discovered that aminoguanidine had greater affinity for hOCT2 than hOCT1, in addition to guanidine and creatinine. Therefore hOCT2 could function as a transporter for aminoguanidine at the basolateral membranes of renal proximal tubules. These findings will be helpful to elucidate the specificity of hOCT2, and clarify the pharmacokinetics of aminoguanidine.

Acknowledgements

This work was supported in part by a grant-in-aid for Research on Biological Markers for New Drug Development, Health and Labour Sciences Research Grants from the Ministry of Health, Labour and Welfare of Japan, by the Mochida Memorial Foundation for Medical and Pharmaceutical Research, and by a grant-in-aid for Scientific Research from the Ministry of Education, Science, Culture and Sports of Japan.

References

[1] Gorboulev V, Ulzheimer JC, Akhoundova A, Ulzheimer-Teuber I, Karbach U, Quester S, et al. Cloning and characterization of two human polyspecific organic cation transporters. DNA Cell Biol 1997;16:871–81.
[2] Zhang L, Dresser MJ, Gray AT, Yost SC, Terashita S, Giacomini KM. Cloning and functional expression of a human liver organic cation transporter. Mol Pharmacol 1997;51:913–21.
[3] Motohashi H, Sakurai Y, Saito H, Masuda S, Urakami Y, Goto M, et al. Gene expression levels and immunolocalization of organic ion transporters in the human kidney. J Am Soc Nephrol 2002;13:866–74.
[4] Inui K, Masuda S, Saito H. Cellular and molecular aspects of drug transport in the kidney. Kidney Int 2000;58:944–58.
[5] Urakami Y, Okuda M, Masuda S, Akazawa M, Saito H, Inui K. Distinct characteristics of organic cation transporters, OCT1 and OCT2, in the basolateral membrane of renal tubules. Pharm Res 2001;18:1528–34.
[6] Grundemann D, Liebich G, Kiefer N, Koster S, Schomig E. Selective substrates for non-neuronal monoamine transporters. Mol Pharmacol 1999;56:1–10.
[7] Urakami Y, Kimura N, Okuda M, Inui K. Creatinine transport by basolateral organic cation transporter hOCT2 in the human kidney. Pharm Res 2004;21:976–81.
[8] Kimura N, Masuda S, Tanihara Y, Ueo H, Okuda M, Katsura T, et al. Metformin is a superior substrate for renal organic cation transporter OCT2 rather than hepatic OCT1. Drug Metab Pharmacokinet 2005;20:379–86.
[9] De Deyn P, Marescau B, Lornoy W, Becaus I, Lowenthal A. Guanidino compounds in uraemic dialysed patients. Clin Chim Acta 1986;157:143–50.
[10] De Deyn PP, Marescau B, Cuykens JJ, Van Gorp L, Lowenthal A, De Potter WP. Guanidino compounds in serum and cerebrospinal fluid of non-dialyzed patients with renal insufficiency. Clin Chim Acta 1987;167:81–8.
[11] Kishore BK, Kallay Z, Tulkens PM. Clinico-biochemical aspects of guanidine compounds in uraemic toxicity. Int Urol Nephrol 1989;21:223–32.
[12] Marescau B, Nagels G, Possemiers I, De Broe ME, Becaus I, Billiouw JM, et al. Guanidino compounds in serum and urine of nondialyzed patients with chronic renal insufficiency. Metabolism 1997;46:1024–31.
[13] Torremans A, Marescau B, Kranzlin B, Gretz N, Billiouw JM, Vanholder R, et al. Biochemical validation of a rat model for polycystic kidney disease: comparison of guanidino compound profile with the human condition. Kidney Int 2006;69:2003–12.
[14] Vanholder R, De Smet R, Glorieux G, Argiles A, Baurmeister U, Brunet P, et al. Review on uremic toxins: classification, concentration, and interindividual variability. Kidney Int 2003;63:1934–43.
[15] Foote EF, Look ZM, Giles P, Keane WF, Halstenson CE. The pharmacokinetics of aminoguanidine in end-stage renal disease patients on hemodialysis. Am J Kidney Dis 1995;25:420–5.
[16] Edelstein D, Brownlee M. Mechanistic studies of advanced glycosylation end product inhibition by aminoguanidine. Diabetes 1992;41:26–9.
[17] Bolton WK, Cattran DC, Williams ME, Adler SG, Appel GB, Cartwright K, et al. Randomized trial of an inhibitor of formation of advanced glycation end products in diabetic nephropathy. Am J Nephrol 2004;24:32–40.
[18] Yokoo S, Masuda S, Yonezawa A, Terada T, Katsura T, Inui K. Significance of organic cation transporter 3 (SLC22A3) expression for the cytotoxic effect of oxaliplatin in colorectal cancer. Drug Metab Dispos 2008;36:2299–306.
[19] Kimura N, Okuda M, Inui K. Metformin transport by renal basolateral organic cation transporter hOCT2. Pharm Res 2005;22:255–9.
[20] Bradford MM. A rapid and sensitive method for the quantitation of microgram quantities of protein utilizing the principle of protein–dye binding. Anal Biochem 1976;72:248–54.

[21] Gibson TP, Matusik EJ, Briggs WA. N-Acetylprocainamide levels in patients with end-stage renal failure. Clin Pharmacol Ther 1976;19:206–12.
[22] Piafsky KM, Borga O, Odar-Cederlof I, Johansson C, Sjoqvist F. Increased plasma protein binding of propranolol and chlorpromazine mediated by disease-induced elevations of plasma alpha1 acid glycoprotein. N Engl J Med 1978;299:1435–9.
[23] Larsson R, Bodemar G, Norlander B. Oral absorption of cimetidine and its clearance in patients with renal failure. Eur J Clin Pharmacol 1979;15:153–7.
[24] Sambol NC, Chiang J, Lin ET, Goodman AM, Liu CY, Benet LZ, et al. Kidney function and age are both predictors of pharmacokinetics of metformin. J Clin Pharmacol 1995;35:1094–102.
[25] Martinez-Gomez MA, Sagrado S, Villanueva-Camanas RM, Medina-Hernandez MJ. Characterization of basic drug-human serum protein interactions by capillary electrophoresis. Electrophoresis 2006;27:3410–9.
[26] Zhang L, Gorset W, Dresser MJ, Giacomini KM. The interaction of n-tetraalkylammonium compounds with a human organic cation transporter, hOCT1. J Pharmacol Exp Ther 1999;288:1192–8.
[27] Bednarczyk D, Ekins S, Wikel JH, Wright SH. Influence of molecular structure on substrate binding to the human organic cation transporter, hOCT1. Mol Pharmacol 2003;63:489–98.
[28] Grundemann D, Hahne C, Berkels R, Schomig E. Agmatine is efficiently transported by non-neuronal monoamine transporters extraneuronal monoamine transporter (EMT) and organic cation transporter 2 (OCT2). J Pharmacol Exp Ther 2003;304:810–7.
[29] Makita Z, Vlassara H, Cerami A, Bucala R. Immunochemical detection of advanced glycosylation end products in vivo. J Biol Chem 1992;267:5133–8.
[30] Shannon JA. The renal excretion of creatinine in man. J Clin Invest 1935;14:403–10.
[31] Miller BF, Winkler AW. The renal excretion of endogenous creatinine in man. Comparison with exogenous creatinine and inulin. J Clin Invest 1938;17:31–40.
[32] Sambol NC, Chiang J, O'Conner M, Liu CY, Lin ET, Goodman AM, et al. Pharmacokinetics and pharmacodynamics of metformin in healthy subjects and patients with noninsulin-dependent diabetes mellitus. J Clin Pharmacol 1996;36:1012–21.
[33] Sirtori CR, Franceschini G, Galli-Kienle M, Cighetti G, Galli G, Bondioli A, et al. Disposition of metformin (N,N-dimethylbiguanide) in man. Clin Pharmacol Ther 1978;24:683–93.
[34] Pentikainen PJ, Neuvonen PJ, Penttila A. Pharmacokinetics of metformin after intravenous and oral administration to man. Eur J Clin Pharmacol 1979;16:195–202.

Journal of Human Genetics (2009) 54, 40–46

www.nature.com/jhg

ORIGINAL ARTICLE

Identification of multidrug and toxin extrusion (MATE1 and MATE2-K) variants with complete loss of transport activity

Moto Kajiwara[1], Tomohiro Terada[1], Ken Ogasawara[1], Junko Iwano[1], Toshiya Katsura[1], Atsushi Fukatsu[2], Toshio Doi[3] and Ken-ichi Inui[1]

H^+/organic cation antiporters (multidrug and toxin extrusion: MATE1 and MATE2-K) play important roles in the renal tubular secretion of cationic drugs. We have recently identified a regulatory single nucleotide polymorphism (SNP) of the *MATE1* gene (−32G>A). There is no other information about SNPs of the *MATE* gene. In this study, we evaluated the functional significance of genetic polymorphisms in *MATE1* and *MATE2-K*. We sequenced all exons of *MATE1* and *MATE2-K* genes in 89 Japanese subjects and identified coding SNPs (cSNPs) encoding MATE1 (V10L, G64D, A310V, D328A and N474S) and MATE2-K (K64N and G211V). All the variants except for MATE1 V10L showed significant decrease in transport activity. In particular, MATE1 G64D and MATE2-K G211V variants completely lost transport activities. When membrane expression level was evaluated by cell surface biotinylation, those of MATE1 (G64D and D328A) and MATE2-K (K64N and G211V) were significantly decreased compared with that of wild type. These findings suggested that the loss of transport activities of the MATE1 G64D and MATE2-K G211V variants were due to the alteration of protein expression in cell surface membranes. This is the first demonstration of functional impairment of the MATE family induced by cSNPs.
Journal of Human Genetics (2009) **54,** 40–46; doi:10.1038/jhg.2008.1; published online 9 January 2009

Keywords: cSNP; H^+/organic cation antiporter; MATE1; MATE2-K; pharmacogenomics; polymorphism; transporter

INTRODUCTION

In the proximal tubules of the mammalian kidney, organic ion transporters limit or prevent the toxicity of organic anions and cations by actively secreting these substances from the circulation into the urine.[1–4] Among human organic ion transporters located at the basolateral membranes, organic cation transporter 2 (OCT2), organic anion transporter 1 (OAT1) and OAT3 were isolated a decade ago, and have been well characterized as key transporters to regulate the renal handling of ionic drugs.[4,5] In contrast, the molecular functions of apical transporters have been only recently characterized. For example, multidrug resistance-associated protein 4 (MRP4) was demonstrated to be responsible for the renal elimination of antiviral drugs,[6] diuretics[7] and cephalosporin antibiotics.[8] Human orthologs of the multidrug and toxin extrusion (MATE) family, members of which confer multidrug resistance on bacteria, were identified most recently,[9,10] and named MATE1 (SLC47A1) and MATE2-K (SLC47A2). Both transporters are expressed mainly in the renal brush border membranes, and are able to transport tetraethylammonium (TEA) utilizing an oppositely directed H^+ gradient as a driving force,[11] indicating that MATE1 and MATE2-K are H^+/organic cation antiporters. These findings have improved the molecular understanding of the transcellular transport of ionic drugs in the renal tubules.

It is widely recognized that there is a large variation in the responses to drugs among individuals. Many enzymes involved in drug metabolism, such as cytochrome *P*450 and uridine diphosphate-glucuronosyltransferase are known to be polymorphic and have been associated with variations in blood concentrations of drugs.[12] In addition to drug-metabolizing enzymes, the clinical significance of genetic variation of drug transporters has been demonstrated.[13] For example, polymorphisms of *SLCO1B1*, which encodes the organic anion transporting polypeptide 1B1 to mediate the hepatic uptake of pravastatin, contribute to the interindividual variability in the disposition of pravastatin.[14] Recent studies of OCT have demonstrated that polymorphisms of the *OCT1* gene in Caucasians and the renal *OCT2* gene in Koreans are responsible for the interindividual differences in the therapeutic efficacy and pharmacokinetics of metformin, an anti-diabetic agent.[15–17]

Metformin showed large interindividual variation in renal clearance, and a potential genetic contribution by the renal transporter was speculated.[18] Because metformin is also a superior substrate for

[1]Department of Pharmacy, Kyoto University Hospital, Kyoto, Japan; [2]Division of Artificial Kidneys, Kyoto University Hospital, Faculty of Medicine, Kyoto University, Kyoto, Japan and [3]Department of Clinical Biology and Medicine, University of Tokushima, Tokushima, Japan
Correspondence: Professor K Inui, Department of Pharmacy, Kyoto University Hospital, Shogoin, Sakyo-ku, Kyoto 606-8507, Japan.
E-mail: inui@kuhp.kyoto-u.ac.jp
Received 13 August 2008; revised 20 October 2008; accepted 3 November 2008; published online 9 January 2009

MATE1 and MATE2-K,[10,19] polymorphisms of *MATE1* and *MATE2-K* genes may be involved in the interindividual difference in the renal clearance. We have recently identified a single nucleotide polymorphism (SNP) in the promoter region of *MATE1* (−32G>A), which causes a decrease in Sp1 binding and promoter activity of approximately 50%.[20] However, other genetic information for these transporters, especially the polymorphisms in the coding region, and their effect on functional properties, have not been well evaluated. In this study, therefore, we screened for polymorphisms in all exons of *MATE1* and *MATE2-K* genes, and examined their transport activities by *in vitro* transient expression system.

MATERIALS AND METHODS

Materials

[^{14}C]TEA bromide (2.035 GBq mmol^{-1}) and [^{14}C]metformin (1.998 GBq mmol^{-1}) were obtained from American Radiolabeled Chemicals Inc. (St Louis, MO, USA) and Moravek Biochemicals Inc. (Brea, CA, USA), respectively. All other chemicals used were of the highest purity available.

Identification of SNPs of *MATE1* and *MATE2-K* genes

Genomic DNA was isolated from peripheral blood from 89 Japanese subjects with renal diseases using a Wizard Genomic DNA Purification Kit (Promega, Madison, WI, USA). Genotyping was investigated by direct sequencing. PCR primers were designed to span all 17 exons of *MATE1* and *MATE2-K* (GenBank accession number NT_010718) (Table 1). The PCR conditions were 94 °C for 3 min, followed by 40 cycles of 94 °C for 30 s, 60 °C for 30 s and 72 °C for 30 s, and then a final extension at 72 °C for 10 min, except for MATE1 exon 1. The condition for MATE1 exon 1 was 94 °C for 1 min, followed by 35 cycles of 94 °C for 30 s and 68 °C for 3 min, and then a final extension at 68 °C for 3 min. The PCR products were sequenced using a multicapillary DNA sequencer RISA384 system (Shimadzu, Kyoto, Japan). This study was conducted in accordance with the Declaration of Helsinki and its amendments and was approved by the Ethics Committee of Kyoto University Graduate School and Faculty of Medicine. All subjects gave their written informed consents.

Construction of non-synonymous variants of MATE1 and MATE2-K

MATE1 and MATE2-K cDNA were excised from MATE1/pcDNA3.1 and MATE2-K/pcDNA3.1,[10] and were subcloned into pcDNA3.1/nV5-DEST (Invitrogen, Carsbad, CA, USA) to yield nV5-MATE1 and nV5-MATE2-K. Non-synonymous variants were constructed by the site-directed mutagenesis of nV5-MATE1 and nV5-MATE2-K, using a QuikChange II Site-Directed Mutagenesis Kit (Stratagene, La Jolla, CA, USA) with the primers listed in Table 2. The nucleotide sequences of these constructs were confirmed using a multicapillary DNA sequencer RISA384 system (Shimadzu).

Transport studies

HEK293 cells (ATCC CRL-1573; American Type Culture Collection) were cultured in complete medium consisting of Dulbecco's modified Eagle's medium (Sigma Chemical Co., St Louis, MO, USA) with 10% fetal bovine serum (Invitrogen) in an atmosphere of 5% CO_2 and 95% air at 37 °C. cDNA plasmid transfection (Figure 2: 25 ng; Figure 3: 100 ng; Figure 6: 100 ng for MATE1 and 200 ng for MATE2-K) and cellular uptake of [^{14}C]TEA and [^{14}C]metformin were reported earlier.[11,19,21,22]

Table 1 Primers used for direct sequencing

Gene	*Location*	*Forward primer (5′ to 3′)*	*Reverse primer (5′ to 3′)*	*Amplified length (bp)*
MATE1	Exon 1	CGCAGTGGTGCAGAGAGAGGTGCAA	AGTCACCCGCGGAGGCAGAAATCAC	451
	Exon 2	AAGGTGGCAGAGGCTCACTGAAGTT	TCTGTGTAGGTTTCAGCCACTACAT	339
	Exon 3	TGAAGGAGGAGCTTTGCAGGCTCTT	CCTGCCAGTGGAGCTCTTCCATCTA	248
	Exon 4	CTTTGTGTGGCACAATTGAAGGCTT	CACCCAGACAGGATAATCTTTCCGT	303
	Exon 5	CTTCTGCCTAACTTTCCCTGGAAAC	CTGAGCTCACAGATATGGTGGCTAC	192
	Exon 6	CTGCCGTGTGACCTCACTTCTGTGT	GGTCCCTGGTCCTGGAGTATCTTCA	208
	Exon 7	GCCTGTGTGTGCTTGGGTAGCAGAA	CGCATGGACACAAGAACCAGCTGAA	279
	Exon 8, 9, 10	ATGAGTCTCCCCTCCTCACTGAGTT	TGCCTGTGCTCATCCATAGACTCTT	633
	Exon 11, 12	ATGAGGCTGCTTCTCTGCACGTGTT	CAGCAATGTTTCTGAACAGCCTGAT	481
	Exon 13	CCACTGCGCCTAGCCAGAAAGCTAT	CCCTCCTCTCAGCTGAAATTTACCA	224
	Exon 14	CTCGGGAGATGGGAGTGTTTCAAGA	AAGACCCGTGTGCTCCGACGGTCAT	276
	Exon 15	CTCCACCTCAGCCATGAAAGCAGAT	AGGGAGAGCCAGATCAGATCCTGTT	289
	Exon 16	TGGCTTGGCTCTTCCTAAACTAGGT	TAGCAGCAAATCTAGCTGTGTCTCA	258
	Exon 17	CTCTCCACTATTAGCACATATTCCTT	ATCCATGGGCACACCTGAATGACAT	436
MATE2-K	Exon 1	CTCATCCCACAAGTTGCCATGGTAG	GCACATTTCTGGATCCTGCCTGCAA	369
	Exon 2	CCTCAAAGCTGGAGAGGCCTGTCTT	GGCTGTGTCTTCCCATCCCTGACCA	297
	Exon 3	GGCACACAGCACATGAGGCTGCTGA	TGCCATCTCCATGGCACCTGTGGAA	292
	Exon 4	TCAGGAAGGCCGCTGTGCCATTACA	TGAGGGCTGGGCATCTTCAGGGTTT	400
	Exon 5	GAGGTTTCACAGTCCTGGCTGAGAC	AGGGATCTTCCGCAGCAGATAGAGT	262
	Exon 6	CAATCTGGGGTACTATGTCCTGGAA	GCTGGTTCACAGATGGTGGAGAGAA	252
	Exon 7	CCTTCTCTCCACCATCTGTGAACCA	CAGGATGGTGACTGATCTGTCTCCA	422
	Exon 8	CCCTGGTTGAGTCTGATCCCAGGAT	TCCAACAGGCTCTACTGCACCCTCT	351
	Exon 9	AATGCCCAGTGCCTGAGCCTGCTAA	TGAGGGCCTGGCCAGTGAAGCTGGAA	403
	Exon 10	TCCCCAAAGCAAAGCAGCGTCCTGT	GGGAGACAGAGATAGCTTCAGGTGA	254
	Exon 11	CTCTTACACTGCATGCCTGAGATCT	TCACAGCAGCAGGGAAGGAGTGAGT	488
	Exon 12	GGCTGGGCTGACTTGCACTGACATA	CCCAGCACTGAGCCAGGAATGTGAT	275
	Exon 13	CTCTGGGCTAGCAGTGCCAGTTACA	CAAGTTCATCCTCACAGCCCTGCGA	317
	Exon 14, 15	TGCCATGCGAATGGCTTAGCACAGT	CTGGGCATTTCTGGCTGAGTAGTCA	483
	Exon 16	CAGTGAAGGGGTGAACTGTTGAGCT	CACAGAGGGCAGACAAGAGCAACAT	225
	Exon 17	CACAGCCAGGTGGTTAACCTAGGTT	ACCTGCACTAGACCCCATTGGTGTT	416

Table 2 Primers used for site-directed mutagenesis

Gene	*Name*	*Direction*	*Sequence (5′-3′)*	*Position*
			Primers for the site-directed mutagenesis	
MATE1	V10L	F	GGAGCCCGCGCCA**T**TGCGCGGAGGCC	15/40
		R	GGCCTCCGCGCA**A**TGGCGCGGGCTCC	40/15
	G64D	F	CCGTGTTCTGTG**A**CCACCTGGGCAAGCTGG	179/208
		R	CCAGCTTGCCCAGGTGG**T**CACAGAACACGG	208/179
	A310V	F	CATGGTCCCTG**T**AGGCTTCAGTGTGGCTGCC	918/948
		R	GGCAGCCACACTGAAGCCT**A**CAGGGACCATG	948/918
	D328A	F	CGCTCTGGGTGCTGGAG**C**CATGGAGCAGG	966/994
		R	CCTGCTCCATG**G**CTCCAGCACCCAGAGCG	994/966
	N474S	F	GGCTCAGGTACACGCCA**G**TTTGAAAGTAAACAACGTGCC	1404/1442
		R	GGCACGTTGTTTACTTTCAAA**C**TGGCGTGTACCTGAGCC	1442/1404
MATE2-K	K64N	F	GGCACCTGGGCAA**T**GTGGAGCTGGC	179/203
		R	GCCAGCTCCAC**A**TTGCCCAGGTGCC	203/179
	G211V	F	GGGGGTCAGGG**T**CTCCGCCTATGCC	621/645
		R	GGCATAGGCGGAG**A**CCCTGACCCCC	645/621

Abbreviations: F, forward; R, reverse.
Mutations introduced into the oligonucleotides are shown in bold.

Table 3 cSNPs of the *MATE1* and *MATE2-K* in 89 Japanese subjects

Location	*SNP*	*dbSNP (NCBI)*	*Effects*	*Allelic frequency (%)*	*Genotype (n)*
MATE1					
Exon1	28G>T	ss104806851	V10L	2.2	G/G 85, G/T 4, T/T 0
Exon1	33C>T	ss104806852	R11R	0.6	C/C 88, C/T 1, T/T 0
Exon1	126T>C	ss104806853	A42A	0.6	T/T 88, T/C 1, C/C 0
Exon2	191G>A	ss104806854	G64D	0.6	G/G 88, G/A 1, A/A 0
Exon8	708C>T	ss104806855	L236L	9.6	C/C 74, C/T 13, T/T 2
Exon11	929C>T	ss104806856	A310V	2.2	C/C 85, C/T 4, T/T 0
Exon11	983A>C	ss104806857	D328A	0.6	A/A 88, A/C 1, C/C 0
Exon16	1421A>G	ss104806858	N474S	0.6	A/A 88, A/G 1, G/G 0
MATE2-K					
Exon2	192G>T	ss104806859	K64N	0.6	G/G 88, G/T 1, T/T 0
Exon2	207G>A	ss104806860	S69S	5.6	G/G 79, G/A 10, A/A 0
Exon4	345C>A	ss104806861	G115G	36.5	C/C 37, C/A 39, A/A 13
Exon8	632_633GC>TT	ss104806862	G211V	1.7	GC/GC 86, GC/TT 3, TT/TT 0
Exon10	885C>T	ss104806863	Y295Y	48.9	C/C 25, C/T 41, T/T 23

Abbreviations: cSNP, coding single nucleotide polymorphism; MATE, multidrug and toxin extrusion.

Cell surface biotinylation

Cell surface biotinylation was performed according to our earlier methods[22] with some modifications. HEK293 cells were grown on poly-D-lysine-coated 12-well plates and transfected with MATE1 or MATE2-K cDNA plasmids (50 ng for MATE1 and 200 ng for MATE2-K). At 48 h after the transfection, cells were washed three times with 1 ml ice-cold phosphate-buffered saline with Ca and Mg (138 mM NaCl, 2.7 mM KCl, 1.5 mM KH_2PO_4, 9.6 mM Na_2HPO_4, 1 mM $MgCl_2$ and 0.1 mM $CaCl_2$, pH 7.3) and then treated with 400 µl of membrane-impermeable biotinylating agent, sulfo-NHS-SS-biotin (Pierce, Rockford, IL, USA) (1.5 mg ml^{-1}) at 4 °C for 1 h. Subsequently, the cells were washed three times with 1 ml ice-cold phosphate-buffered saline with Ca and Mg containing 100 mM glycine and then incubated for 20 min at 4 °C with the same buffer to remove the remaining labeling agent. After being washed with phosphate-buffered saline with Ca and Mg, cells were disrupted with 400 µl of lysis buffer (10 mM Tris-base, 150 mM NaCl, 1 mM EDTA, 0.1% SDS, 1% Triton X-100 and 1% protease inhibitor cocktail (Nacalai Tesque, Kyoto, Japan), pH 7.4) at 4 °C for 1 h with constant agitation. Following centrifugation, 50 µl of streptavidin agarose beads (Pierce) was added to 300 µl of cell lysate and incubated for 1 h at room temperature to isolate the biotinylated membrane proteins.

Western blot analysis and quantification of band density

Isolated biotinylated membrane proteins were subjected to western blot analysis according to NuPAGE manufacturer's instructions (Invitrogen). Monoclonal anti-V5 antibody (Invitrogen) (1:2500 dilution) or Na^+/K^+-ATPase antibody (1:10 000 dilution; Upstate Biotechnology, Lake Placid, NY, USA) was used as the primary antibody. A peroxidase-conjugated anti-mouse IgG antibody was used for the detection of bound antibodies, and the blots were visualized by chemiluminescence on X-ray film. Quantification of band density was performed on scanned images using ImageJ, a public domain image-processing program (W Rasband, National Institute of Mental Health, Bethesda, MD, USA). The optical density of each lane was plotted, and the area under the curve was measured.

Statistical analysis

Kinetic parameter data were statistically analyzed with unpaired *t*-test compared with the values for the wild type. The other experimental data were statistically analyzed with the one-way analysis of variance followed by Dunnett's test.

RESULTS

Identification of *MATE1* and *MATE2-K* SNPs

All 17 exons of the *MATE1* and *MATE2-K* genes were sequenced to find SNPs in 89 Japanese subjects. In this study, eight *MATE1* SNPs and five *MATE2-K* SNPs were identified in the coding region (Table 3). The allelic frequencies for the non-synonymous SNPs ranged from 0.6 to 2.2%. Figure 1 shows the position of mutated amino-acid residues in the predicted secondary structure of MATE1 (a) and MATE2-K (b), respectively. Only Ala310 was localized in the transmembrane domain (TMD), and other amino-acid residues are located at the intra- or extracellular domains.

Transport studies of the MATE1 and MATE2-K variants

To assess the functional alterations caused by the non-synonymous SNPs of both genes, [^{14}C]TEA transport activity by the variants was evaluated by *in vitro* transient expression system. As shown in Figure 2a, [^{14}C]TEA uptake by the MATE1 G64D variant was completely abolished. Other MATE1 variants except for the MATE1 V10L variant also showed a significant reduction in [^{14}C]TEA transport activity, and the order of the remaining transport activities were as follows: wild type=V10L>N474S>D328A=A310V. [^{14}C]Metformin uptake by various variants was similar to [^{14}C]TEA uptake (Figure 2b). Both the MATE2-K variants showed significant decrease in [^{14}C]TEA and [^{14}C]metformin uptake, and the transport activity of MATE2-K G211V was completely abolished (Figures 3a and b).

Cell surface expression levels of the MATE1 and MATE2-K variants

To determine whether the reduced transport activity of these variants was due to the decreased expression of transporter proteins in the plasma membranes, cell surface biotinylation followed by western blot analysis was carried out. Among the MATE1 variants, the cell surface expression level of MATE1 G64D and D328A showed a decrease to approximately 10 and 20% compared with that of the wild-type MATE1 (Figure 4), which are well correlated with the reduction ratios of the transport activity for these variants (Figures 2a and b). Other MATE1 variants exhibited similar cell surface expression level with wild-type MATE1. In the MATE2-K, both the MATE2-K K64N and MATE2-K G211V variants showed a decrease to approximately 50 and 1% compared with that of the wild-type MATE2-K, respectively (Figure 5). These reduction ratios were well correlated with those of transport activities of both the MATE2-K variants (Figures 3a and b). These findings suggested that the low transport activities of MATE1 G64D, D328A and two MATE2-K variants were due to the alteration of protein expression in cell surface membranes.

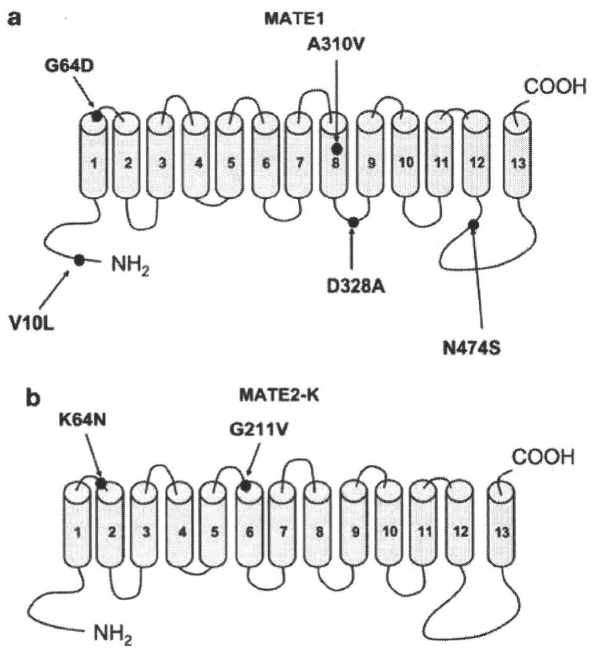

Figure 1 Locations of mutated amino-acid residues caused by non-synonymous single nucleotide polymorphisms (SNPs) in the secondary structure of multidrug and toxin extrusion 1 (MATE1) (**a**) or MATE2-K (**b**) protein. Amino-acid numbers are shown.

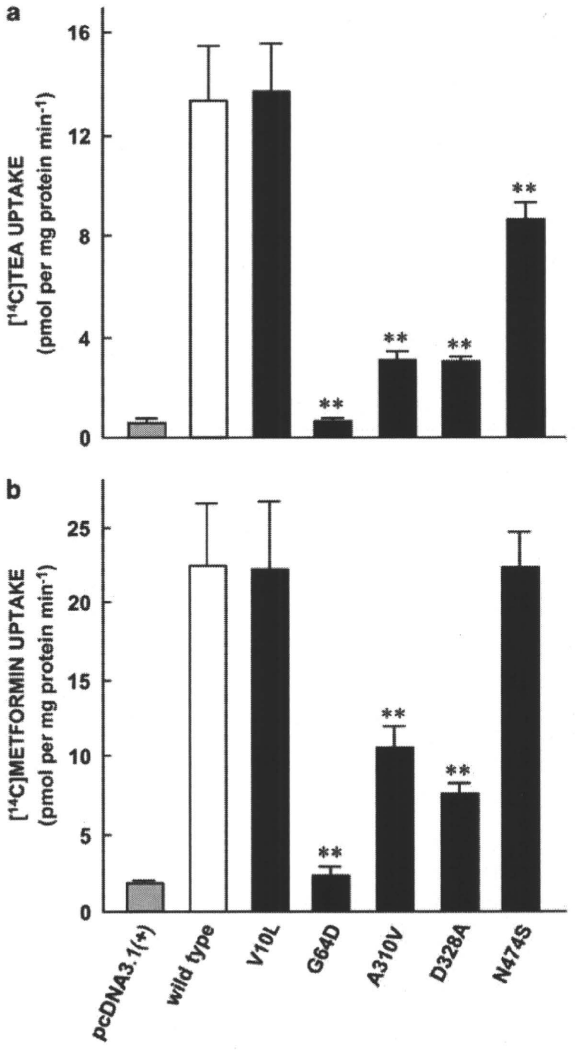

Figure 2 Uptake of [^{14}C]TEA (tetraethylammonium) (**a**) and [^{14}C]metformin (**b**) by HEK293 cells transiently expressing wild type or various multidrug and toxin extrusion 1 (MATE1) variants. The cells were preincubated with incubation medium (pH 7.4) in the presence of 30 mM ammonium chloride for 20 min. Then, the preincubation medium was removed, and the cells were incubated with 5 μM of [^{14}C]TEA or 10 μM of [^{14}C]metformin for 1 min at 37 °C. Each column represents the mean ± s.d. of six monolayers from two independent experiments. $^{**}P<0.01$, significantly different from the values for the wild type.